Temporal Gene Expression Analysis Reveals a Synergistic Effect of Combined Drought and Heat Stress in Grapevine (*Vitis vinifera* L.)

By

Yikang Hu

A thesis submitted for the partial fulfilment of the requirements of the Master of Biotechnology (Plant Biotechnology)

The University of Adelaide

Faculty of Sciences

School of Agriculture, Food & Wine

Waite Campus

2017

Declaration

I declare that this thesis is a record of original work and contains no material which has been accepted for the award of any other degree or diploma in any university. To the best of my knowledge and belief, this thesis contains no material previously published or written by another person, except where due reference is made in the text.

_____ _____

Yikang Hu Date

Contents

Preface

This research was performed over 10 months as part of a Master of Biotechnology (Plant Biotechnology). In accordance with the requirements of the program, the research is presented in the format of a manuscript for submission to a peer-reviewed scientific journal. I have chosen to follow the format of *Journal of Experimental Botany*. My co-authors for the manuscript are Carlos Rodriguez Lopez, Kiflu Gebremicael Tesfamicael, Penny Tricker, Ute Baumann and Everard Edwards. Carlos Rodriguez Lopez developed the novel experimental design that I used in this research and supervised me in the other aspects of the data analysis. Kiflu Gebremicael Tesfamicael helped to carry out the glasshouse experiment and assisted me with lab experiment and data collection. Na Sai, Konstantinos Bogias and Jimmy Breen helped me with bioinformatics application. Carlos Rodriguez Lopez suggested the project, supervised my research and reviewed drafts of the manuscript. The manuscript in this thesis is intended as the first draft of a manuscript for future publication. The final word count for the manuscript (excluding references and supplementary materials) is 7804.

The appendix contains the supplementary materials. I have followed the Author Guide except that I used double-spaced line and lack of line numbering for which my manuscript differs from the journal's instructions to satisfy the thesis guidelines for the Master of Biotechnology (Plant Biotechnology) program.

Research Manuscript

Title: Temporal Gene Expression Analysis Reveals a Synergistic Effect of Combined Drought and Heat Stress in Grapevine (*Vitis vinifera* L.)

Author: Yikang Hu[1]

Co-author: Carlos Rodriguez Lopez[1], Kiflu Gebremicael Tesfamicael[1], Penny Tricker[2], Ute Baumann[2] and Everard Edwards[1].

[1]Environmental Epigenetics and Genetics Group, School of Agriculture, Food and Wine, the University of Adelaide, South Australia.

[2]Plant Genomics Centre, School of Agriculture, Food and Wine, the University of Adelaide, South Australia.

Yikang Hu

Email: a1680625@student.adelaide.edu.au

Carlos Rodriguez Lopez

Email: carlos.rodriguezlopez@adelaide.edu.au

Kiflu Gebremicael Tesfamicael

Email: kiflu.tesfamicael@adelaide.edu.au

Penny Tricker

Email: penny.tricker@adelaide.edu.au

Ute Baumann

Email: ute.baumann@adelaide.edu.au

Everard Edwards

Email: everard.edwards@adelaide.edu.au

Abbreviations

Abscisic Acid (ABA)

Counts Per Million (CPM)

Diethylpyrocarbonate (DEPC)

Differentially Expressed Genes (DEGs)

False Discovery Rate (FDR)

Gene Ontology (GO)

Hierarchical Indexing for Spliced Alignment of Transcripts (HISAT)

Log Ration Fold Change (LogFC)

Nitric Oxide (NO)

Nitrate Reductase (NR)

Reactive Oxygen Species (ROS)

Ribosomal RNA (rRNA)

RNA Quality Indicator (RQI)

RNA Sequencing (RNA-Seq)

Vapour Pressure Deficit (VPD)

Abstract

Grapevine (*Vitis vinifera* L. cv. Cabernet Sauvignon) is widely used for winemaking all over the world. Drought and heat stresses are two of the major abiotic stresses reducing grape quality and yield. However, drought and heat tolerance are still poorly characterized in perennial crops such as grapevine. During this study, stomatal conductance, stem water potential and leaf temperature were measured to determine plant physiological status. RNA-seq technology was used for the analysis of differentially expressed genes (DEGs) of leaf samples between the control and three treatments, which were drought, heat and a combined treatment. Gene expression profiles were grouped by treatments and timepoints. The great majority of unique DEGs were found to be induced by the combined drought and heat treatment. 169 up-regulated genes were induced by drought, 85 by heat and 1218 by the combined treatment; 78 down-regulated genes were induced by drought, 72 by heat and 1427 by the combined treatment. Three potential and significant regulation pathways of stress response were identified based on Gene Ontology (GO) analysis i.e. cytokinin-activated signalling pathway, ion transport pathway and Nitric Oxide-mediated pathway. This study provides preliminary insights into the transcriptomic response to drought and heat stress in grapevine.

Key words: Grapevine, RNA-seq, Drought, Heat, Differentially Expressed Genes, Gene Ontology

1. Introduction

Grapevine (*Vitis vinifera* L. cv. Cabernet Sauvignon) is vital for winemaking and of great significance in Australia. Over the past two decades, Australia has grown rapidly to be one of the major wine producing countries in the New World. South Australia, with over 40% of the total Australian production (Fuentes *et al.*, 2013), is the main grape growing region as well as the main wine producing state in Australia (Soosay and Andrew, 2011; Fuentes *et al.*, 2013). Wine exports of South Australia form a significant part of the state's economy, accounting for about 63% of the national wine exports (Fuentes *et al.*, 2013).

Grape production practices are particularly vulnerable to issues related to climate change. The average temperature in most regions over the world has risen by 1-3 ºC over the last 50 years (Dai, 2011). Even a conservative prediction of a 2 ºC rise of the globally averaged temperature may cause a rise of sea levels, heavy rainfall or intense drought, heat waves, tornados and other extreme weather events (Kang and Banga, 2013). In Mediterranean climate regions, such as wine producing regions in Australia, grapevines grow in a seasonal environment with long hot and dry summers (Chaves *et al.*, 2010; Ben Salem-Fnayou *et al.*, 2011; Carvalho *et al.*, 2015). The predicted climate change will lead to more stress in Mediterranean climate regions. Drought stress is characterized by the decline in rainfall and increase in average maximum temperature (Garnaut, 2008). In other words, heat stress is commonly combined with drought, influencing grapevine growth and development. For this reason, it is expected that the main future challenge to the viticulture industry will be the occurrence of more frequent and widespread drought and heat stress (Bandurska *et al.*, 2017).

Climate change is already impacting the grape and wine community in Australia. For instance, Australian vineyards are reaching veraison earlier (Soar *et al.*, 2008) and vintages have advanced by 5-10 days in the last 15 years (Araus and Slafer, 2011). In 2007, Australia experienced the worst drought in the last 30 years, and wine production reduced 25% at that time (Soosay and Andrew, 2011). Abiotic stresses not only reduce yield but also affect berry size and flavour (Cramer, 2010). Such changes further affect wine quality, including aroma, colour and intensity (Mira de Orduña, 2010). The wine industry has encountered great pressure due to the various effects of climate change and may be under greater pressure with the predicted climate change situation. Cabernet Sauvignon budburst in Coonawarra of SA is expected to happen earlier by four to eight days in 2030, and by six to eleven days in 2050 (Webb *et al.*, 2007). Climate change is predicted to produce a 44% decrease in land suitable for grape production by 2050 in Australia (Garnaut, 2008). Because of the expected warming, several grape-producing regions in Australia will be unsuitable for premium wine production in the future (Hall and Jones, 2009). Moreover, the drought and heat crisis will also cause a higher water demand in the future. Water scarcity has already become a global problem, and the situation of water shortage in Australia is severe (Moore *et al.*, 2011). For example, years of drought exerted major constraints on the sustainable production and resilience of Australian vineyards between 2006 and 2009, as water allocation was reduced to as low as 18% of normal allocation levels (Phogat *et al.*, 2017). Therefore, understanding how grapevine copes with drought and heat stress is paramount.

Under stress conditions, plants respond commonly by expressing specifically functional genes to protect themselves. The stress-related genes play a crucial role in stress response as well as plant development. Currently, RNA-seq (RNA sequencing) technology is a suitable and developed approach to study the gene expression regulations and to uncover the potentially molecular mechanisms. To date, Sun et al. (2014) showed that the number of down-regulated genes was far more than that of up-regulated genes in *Chrysanthemum nankingense* (Asteraceae) under heat stress. Some biological processes were suppressed by heat stress, such as RNA polymerase, RNA methyltransferase, pre-mRNA splicing factor and RNA helicase. Through transcriptome analysis, the gene expression of drought-tolerant barley was more conserved in evolution than that of the sensitive wild barley (Hübner *et al.*, 2015). In rice floral organs, RNA-seq analysis revealed that genes involved in pectinase biosynthesis were highly responsive to heat stress (Wu *et al.*, 2015). Magalhães et al. (2015) utilised the RNA-seq approach to construct a gene network of abscisic acid (ABA)-signalling pathway associated with the drought tolerance. Chen et al. (2016) found that the differential expression under heat stress was regulated at both transcriptional and post-transcriptional level. The gene expression of splicing factors showed that the changes of alternative splicing were in response to drought stress in maize (Thatcher *et al.*, 2016). RNA-seq was used to investigate the effect of sequential biotic and abiotic stresses on the transcriptome dynamics in Arabidopsis (Coolen *et al.*, 2016).

However, most RNA-seq studies focus on model plants (e.g. *Arabidopsis thaliana*), and annual crops such as wheat, rice, corn. Drought and heat tolerance are still poorly characterized in perennial crops such as grapevine. Here, this study aims to identify the differentially expressed

genes (DEGs) in grapevine associated with drought stress, heat stress as well as a combined drought and heat stress. Gene Ontology (GO) analysis of DEGs was performed to reveal the potential and prominent pathways related to stress tolerance. This work contributes to a deeper understanding of the molecular background of drought and heat tolerance in grapevine. Additionally, this study gives a new insight into the transcriptomic response to the combined drought and heat stress in grapevine.

2. Materials and Methods

2.1 Plant Materials and Experimental Design

120 callused dormant cuttings propagated from 6 donor grapevine (*Vitis vinifera* L. Cabernet Sauvignon) plants were planted (25/11/2016) with soil UC mix and maintained in a plant propagator under high humidity until establishment. Plants were then transferred (01/2017) to 24cm pots and randomly allocated into four different groups (i.e. Control (T0), drought (T1), heat (T2) and combined drought and heat (T3)) with a five-replicated block design (Fig. 1) in a glasshouse under controlled conditions for acclimation until treatment (CSIRO, Waite Campus, Adelaide, South Australia, Australia). There were six sampling times in this study (Table 1). Leaf samples and physiological information were collected during the experiment as described in Fig. 2 and 3.

Drought treatment was applied to selected plants (T1 and T3, 15/02/2017) by removing watering drippers. After ten days of drought stress (26/02/2017), heat stress was performed for two consecutive days by the glasshouse air-conditioning system to elevate the temperature. Those plants that were not selected to be under heat stress (i.e. T0 and T1) were moved to a glasshouse with the same layout but controlled temperature (Fig. 1). After heat treatment, plants (T0 and T1) were transferred back to the initial glasshouse and watering was reinitiated for drought-treated plants (28/02/2017).

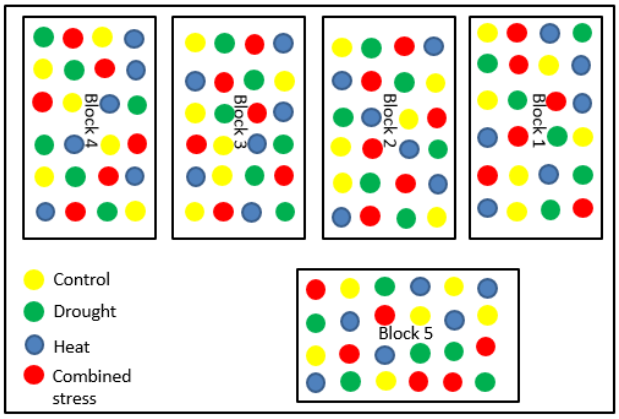

Fig. 1. Schematic diagram of glasshouse layout. Colour code indicates the four treatments and the distribution of grapevine plants in a five-block design: yellow=control (T0); green=drought treatment (T1); blue=heat treatment (T2) and red=combined drought and heat treatment (T3).

Table 1. List of six sampling times

Sampling times	Abbr.	Description
1	ST1	1st day Plant acclimation to glasshouse
2	ST2	1st day of drought treatment
3	ST3	11th day of drought treatment and 1st day of heat treatment
4	ST4	12th day of drought treatment and 2nd day of heat treatment
5	ST5	Day of stress removal
6	ST6	Plant physiological recovery, 16 days after removal of stress treatments

2.2 Plant Phenotyping

2.2.1 Stomatal conductance measurement

Stomatal conductance was measured on the first fully expanded leaves (Fig. 2) using AP4 Leaf Porometer (Delta-T Devices, UK). Stomatal conductance measurement (Meggio *et al.*, 2014) was performed daily during the afternoon (3-4pm) from the initiation of drought treatment until plant physiological recovery (Fig. 3).

2.2.2 Stem water potential

In order to determine the grapevine water status during treatment, stem water potential (Meggio *et al.*, 2014) was measured on the second fully expanded leaf (Fig. 2) of plants selected for tissue sampling at each sampling time (Table 1, Fig. 3) using a Scholander-type pressure

chamber (model 3000, USA). Before measurement, the measured leaves were artificially prevented from light for 30 mins by covering the leaves with aluminium bags (Choné, 2001).

2.2.3 Leaf temperature

In order to determine the effect of high temperature on the grapevine, leaf temperature was measured on the surface of the third young leaf and first fully expanded leaf (Fig. 2) of plants selected for tissue sampling at each sampling time (Table 1, Fig. 3) using a non-contact infrared thermometer (Fluke, USA).

2.2.4 Sample collection

The second and third youngest leaves (Fig. 2) from plants selected for sampling at each sampling time (Table 1, Fig. 3) were collected and immediately frozen in liquid nitrogen and then stored at -80°C until total RNA extraction.

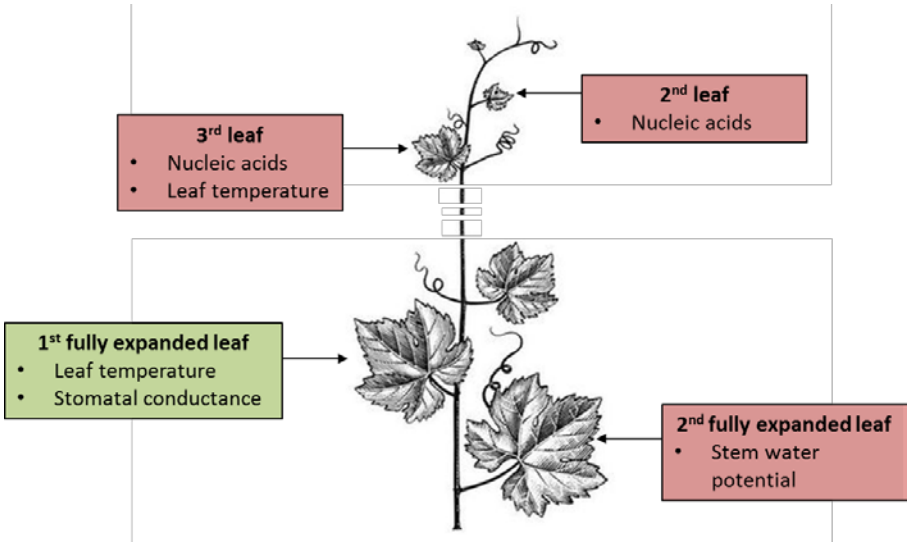

Fig. 2. Physiological data acquisition and sampling strategies. Boxes indicate what measurement was performed on different leaves. Green and red colours indicate non-destructive and destructive sampling approaches respectively.

2.3 Total RNA Extraction

Total RNA was extracted from 100 mg of frozen and ground powder of the second and third youngest leaves from each plant using the Spectrum™ Plant Total RNA Kit (Sigma, St. Louis, Missouri, USA) according to the manufacturer's Protocol A. RNA samples were resuspended in 42 ul of RNase-free DEPC water (Sigma, St. Louis, Missouri, USA). RNA quality and quantity were determined by spectrophotometric analysis (NanoDrop™ 1000, Thermo Fisher Scientific, Wilmington, DE, USA) and Experion™ RNA StdSens Chips (BIO-RAD, USA). Only samples showing nanodrop 260/280 and 260/230 absorbance ratios between 1.8-2.2 and RNA quality indicator (RQI) above 7 were kept for analysis. RNA samples were stored at -80°C until ribosomal depletion.

2.4 Ribosomal Depletion of mRNA

4 ug of total RNA from each sample was used for ribosomal depletion by Dynabeads® mRNA Purification Kit following the manufacturer's instruction (Thermo Fisher Scientific, USA). Captured mRNA samples were resuspended in 15 ul of RNase-free DEPC water.

2.5 Library Preparation and Illumina Sequencing

5 ul ribosomal depleted RNAs were used to prepare RNA-seq libraries using the NEBNext® Ultra™ RNA Library Prep Kit for Illumina (New England Biolabs, USA) following manufacturer’s instructions with some modifications. In brief, during the step 5 of “first strand cDNA synthesis”, samples were incubated at 42°C for 50 minutes. AMPure XP Beads (Beckman Coulter, USA) were used for the purification of the double-stranded cDNA, the

ligation reaction and the PCR reaction. cDNA library size and quality were estimated using 1K Experion™ DNA High Sensitivity Chips (BIO-RAD, USA). Individual library molarity was estimated using average fragment size from Experion reads and sample DNA concentration calculated by Qubit® dsDNA HS Assay Kits (Thermo Fisher Scientific, Wilmington, DE, USA). Finally, individually indexed libraries were diluted to 10nM and pooled prior sequencing. The Illumina NextSeq 500 HighOutPut platform was used to produce 75bp single-end runs at the Australian Genome Research Facility (AGRF) in Adelaide.

2.6 Bioinformatics Analysis

2.6.1 RNA-seq data analysis

Raw sequencing data were processed on Phoenix platform. AdapterRemoval (Lindgreen, 2012) was used for removing adaptors of the raw reads. Sequence quality control was performed with a set of quality checks in FastQC format (https://biof-edu.colorado.edu/videos/dowell-short-read-class/day-4/fastqc-manual). Subsequently, the alignment tool (HISAT2) (Kim *et al.*, 2015; Khalil-Ur-Rehman *et al.*, 2017) was used for mapping the sequencing reads to a 12X grapevine genome reference. The GTF reference of *Vitis vinifera* genome was used for this study from *Ensembl Plants* website (http://plants.ensembl.org/Vitis_vinifera/Info/Index).

2.6.2 Differentially expressed genes (DEGs) analysis

To estimate expression levels, further analysis was processed on RStudio using the *edgeR* package (Robinson *et al.*, 2010). The raw mapped data of each sample was standardized by counts per million (CPM) and genes showing lower than 1 were removed. Subsequently, the filtered data was normalised for differential expression analysis as described previously (Lun *et al.*, 2016). Between control and each treatment, a false discovery rate adjusted P-value<0.01 was adopted to determine differential expression using Benjamini and Hochberg's algorithm. The heat maps of gene expression pattern in drought, heat and drought/heat treatments were performed using the "*pheatmap*" package on RStudio (Wang *et al.*, 2010).

2.6.3 Gene ontology (GO) analysis

To interpret and classify the DEGs associated with drought, heat and drought/heat stress, GO analysis was performed with the "*biomaRt"* package on RStudio (https://cran.r-project.org/web/packages/biomartr/vignettes/Functional_Annotation.html). GO analysis was performed using DEGs on each treatment to attain the significant GO terms (http://web.mit.edu/~r/current/arch/i386_linux26/lib/R/library/limma/html/goana.html). P-value<0.05 was used for the observation probability calculated by the hypergeometric distribution (http://mathworld.wolfram.com/HypergeometricDistribution.html). A Web tool "REVIGO" was used to summarize and visualize the long lists of GO terms (Supek *et al.*, 2011).

3. Results

3.1 Environmental Conditions during Stress Treatment

During 2-day heat treatment, vapour pressure deficit (VPD) and air temperature of heat treatment (orange curves) were both higher than those of the control (grey and blue curves) (Fig. 3A&B). The curve of stomatal conductance of drought-treated plants, as a representative, shows the corresponding sampling times (1-6) (Fig. 3C).

3.2 Physiological Analysis during Drought and Heat Treatment

3.2.1 Stomatal conductance (G_s)

Stomatal conductance differences between control and stressed (drought, heat and drought/heat) plants varied depending on the stress and the sampling times measured. At ST2 (i.e. 1st day of drought treatment), no significant differences were observed between control and drought-treated plants. At ST3 (11th day of drought stress and 1st day of heat treatment), heat-treated plants showed significantly higher G_s than control plants (Fig. 4; t-test, $P<0.01$). On the contrary, plants under drought and drought/heat conditions significantly reduced their G_s by approximately 90% (Fig. 4; t-test, $P<0.01$). At ST4 (12th day of drought stress and 2nd day of heat treatment) heat-treated plants showed no significant differences in G_s when compared to control plants (Fig. 4), while plants under drought and drought/heat conditions maintained the observed reduction in stomatal conductance at ST4 (Fig. 4; t-test, $P<0.05$). No significant differences in G_s were observed at any time point between drought and drought/heat plants (Fig. 4). After the removal of stresses at ST5, the G_s of plants under heat stress showed a significantly higher level of stomatal conductance than control plants (Fig. 4; t-test, $P<0.05$), while those

under drought and drought/heat stress did not show any significant differences. Stressed plants recovered gradually until achieving previous levels at ST 6 (16 days after removal of both stresses) (Fig. 4).

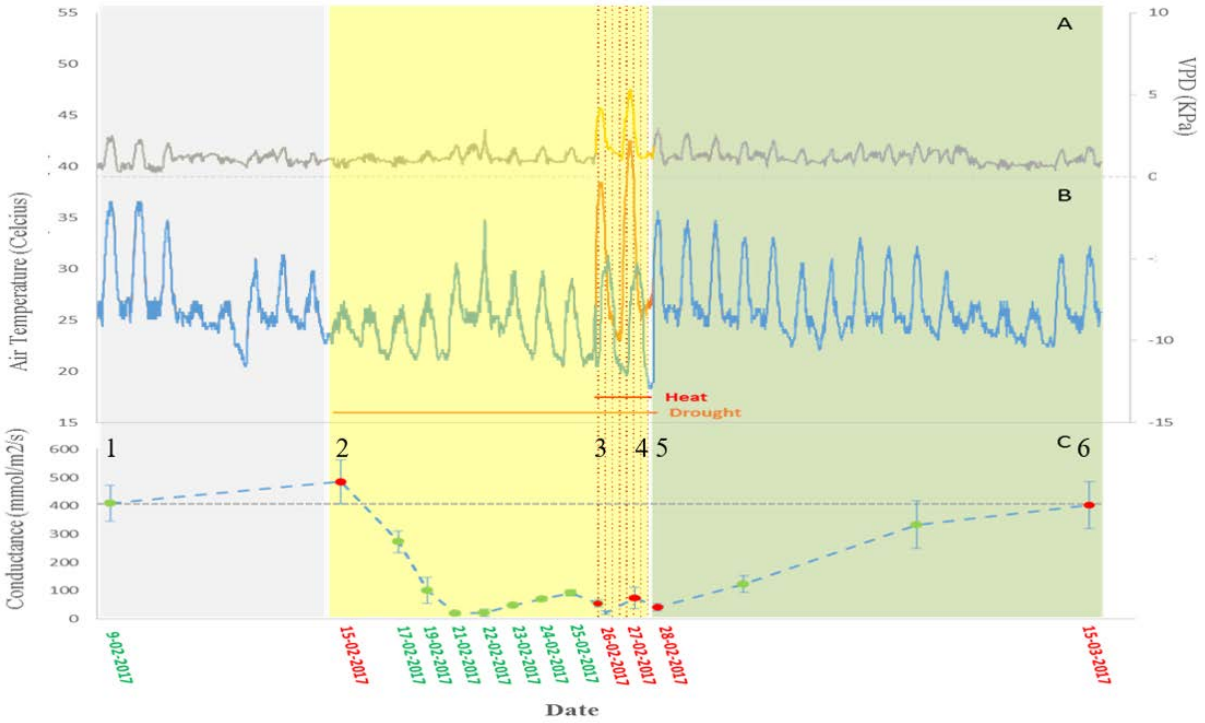

Fig. 3. Stress conditions and corresponding sampling times. (A) Vapour Pressure Deficit (VPD), (B) Air temperature and (C) Stomatal conductance under drought stress. Coloured boxes represent the different stages of this experiment (i.e. grey=plant growth in the normal glasshouse conditions; yellow=drought treatment (orange curves represent the heat treatment during the drought stress period); green=physiological recovery of stressed plants. The number indicates the six sampling times. (A) Grey and orange curves represent VPD measurements (in Kilo Pascals) in the glasshouse under controlled temperature and heat stress conditions, respectively. (B) Blue and orange curves represent the air temperature measurements (in Degree Celsius) in the glasshouse under control temperature and heat stress conditions, respectively. (C) Stem stomatal conductance was regularly measured during treatment. Each dot corresponds to the measurement time.

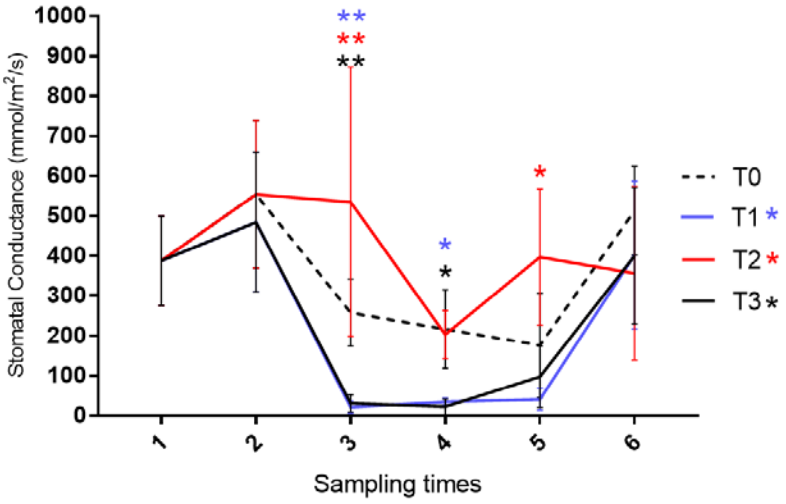

Fig. 4. Variation of stomatal conductance in grapevine during exposure to stresses. Stomatal conductance (G_s) measurements of the control (T0), drought treatment (T1), heat treatment (T2) and a combined drought/heat treatment (T3) at six sampling times. **1**, 1st day plant acclimation to glasshouse; **2**, 1st day of drought treatment; **3**, 11th day of drought stress and 1st day of heat treatment; **4**, 12th day of drought stress and 2nd day of heat treatment; **5**, Day of stress removal; **6**, 16 days after removal of stress treatments. The *t*-test between control and treatments within a sampling time are indicated as *P<0.05 and **P<0.01. Blue asterisk indicates the significance between control and drought treatment; Red asterisk indicates the significance between control and heat treatment; Black asterisk indicates the significance between control and drought/heat treatment.

3.2.2 Stem water potential (stemΨ)

Stem water potential shows a direct effect of drought and heat stress on the grapevine water status (Fig. 5). In brief, stemΨ value reaches close to zero, which means plants hold more water. The stemΨ of control plants stayed at around -0.4 MPa during all the experiment stages. At ST 2 (i.e. 1st day of drought treatment), a significant decline in stemΨ was observed in drought-treated plants (Fig. 5; t-test, $P<0.05$). During drought and heat treatment (ST3, ST4), the stemΨ of the single heat-treated plants experienced a significant decrease (Fig. 5; t-test, $P<0.001$), from -0.4 MPa to -0.75 MPa. The stemΨ of the single drought-treated plants continue to decline from -0.57 MPa to -0.76 MPa, showing the significant difference from control (Fig. 5; t-test, $P<0.001$). Plants under drought/heat treatment showed the lowest stemΨ at approximately -0.97 MPa (Fig. 5; t-test, $P<0.001$). After stress removal at ST 5, the stemΨ of heat-treated plants showed no significant difference (Fig. 5). However, the stemΨ of drought-treated plants and drought/heat-treated plants was still significantly different from that of control at ST5 (Fig. 5; t-test, $P<0.001$). At ST6, no significant differences in stemΨ were observed between the treated plants and control (Fig. 5).

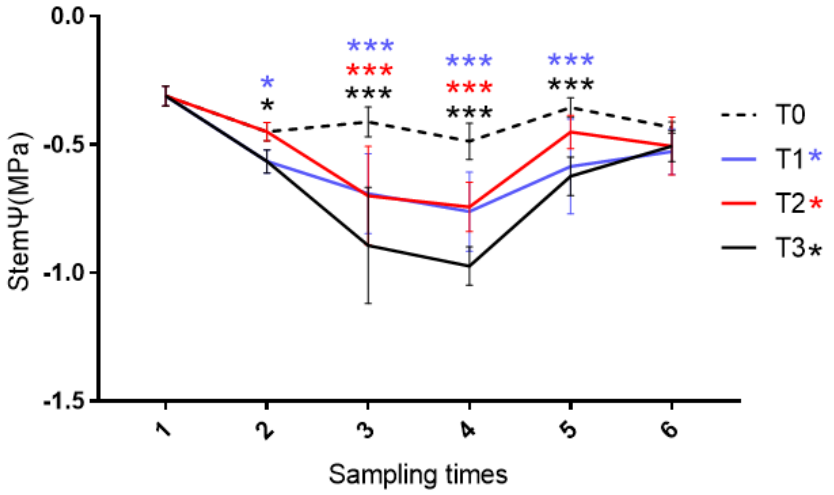

Fig. 5. Variation of stem water potential in grapevine during exposure to stresses. Stem water potential (StemΨ) measurement of the control (T0), drought treatment (T1), heat treatment (T2) and a combined drought/heat treatment (T3) at six sampling times. **1**, 1st day plant acclimation to glasshouse; **2**, 1st day of drought treatment; **3**, 11th day of drought stress and 1st day of heat treatment; **4**, 12th day of drought stress and 2nd day of heat treatment; **5**, Day of stress removal; **6**, 16 days after removal of stress treatments. The *t*-test between control and treatments within a sampling time are indicated as *P<0.05, **P<0.01 and ***P<0.001. Blue asterisk indicates the significance between control and drought treatment; Red asterisk indicates the significance between control and heat treatment; Black asterisk indicates the significance between control and drought/heat treatment.

3.2.3 Leaf temperature

No significant differences were observed in leaf temperature between drought-treated plants and control at all six sampling times (Fig. 6). However, some different situations were observed between the heat-treated and drought/heat-treated plants. At ST2 (i.e. first day of drought treatment), no significant differences were displayed between control and treatments (Fig. 6). At ST3 (11th day of drought stress and 1st day of heat treatment), the leaf temperatures of both third young leaf and first fully expanded leaf showed significant differences between control and drought/heat treatment (Fig. 6; t-test, $P<0.001$). However, heat-treated plants showed significant difference only in the third young leaf (Fig. 6A; t-test, $P<0.001$). At ST4 (12th day of drought stress and 2nd day of heat treatment), the leaf temperatures continued to go up under heat stress. The third young leaf temperature of heat-treated and drought/heat-treated plants peaked at 38.1°C and 40°C, respectively (Fig. 6A). Meanwhile, the first fully expanded leaf temperature of heat-treated and drought/heat-treated plants peaked at 36.1°C and 42°C, respectively (Fig. 6B). At ST5 (Day of stress removal), the third young leaf temperature of heat-treated plants decreased significantly (Fig. 6A) and no significant differences were observed between other treatments and control. At ST6, the leaf temperature of all plants was around 30°C, showing no significant differences. The young leaves' temperature reflected directly the effect of high temperature during heat stress.

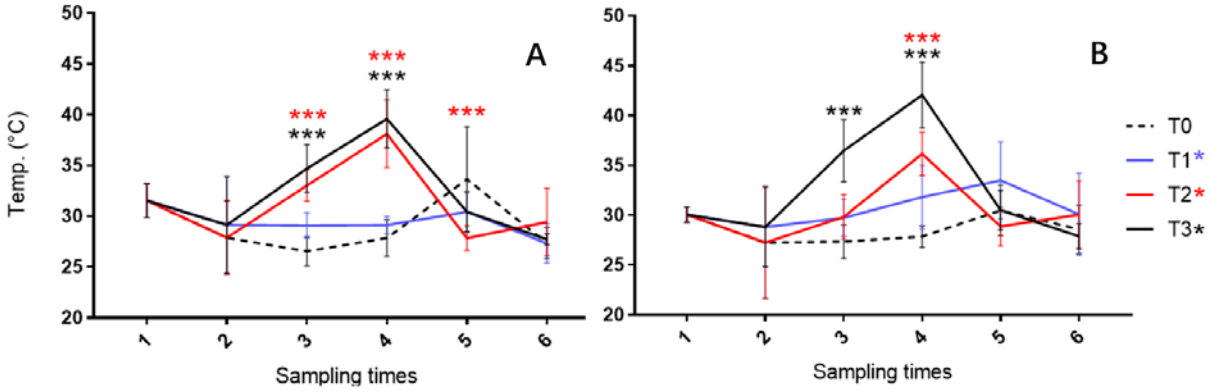

Fig. 6. Variation of leaf temperature in grapevine during exposure to stresses. Leaf temperature measurement of the third young leaf (A) and the first fully expanded leaf (B) from the control (T0), drought treatment (T1), heat treatment (T2) and a combined drought/heat treatment (T3) at six sampling times. **1**, 1st day plant acclimation to glasshouse; **2**, 1st day of drought treatment; **3**, 11th day of drought stress and 1st day of heat treatment; **4**, 12th day of drought stress and 2nd day of heat treatment; **5**, Day of stress removal; **6**, 16 days after removal of stress treatments. The *t*-test between control and treatments within a sampling time are indicated as *P<0.05, **P<0.01 and ***P<0.001. Blue asterisk indicates the significance between control and drought treatment; Red asterisk indicates the significance between control and heat treatment; Black asterisk indicates the significance between control and drought/heat treatment.

3.2 Analysis of RNA-seq Libraries

RNA-seq libraries were prepared from mRNA obtained from 95 samples (Five samples per timepoint/treatment). More specifically, sampling time 1 contained five control samples. Sampling time 2 contained five control samples and five drought-treated samples. Other sampling times contained five samples for each group (control, drought, heat and combined treatment). Of the 95 individual RNA-seq libraries, 84 libraries generated above 18,000,000 reads and were selected for further analysis. An average 85% of the reads were mapped to the *Vitis vinifera* genome database.

3.3 Multidimensional Scaling (MDS) Analysis

Multidimensional scaling (MDS) was used to visualize the global difference and similarity in gene expression pattern. MDS plot showed that the gene expression grouped samples by treatments and by sampling times (Fig. 7). Control plants, during treatment (brown, green, aquamarine and blue circles) and after treatment (ST6, magenta circle and all symbols) occupied the top quadrants of the MDS plot. Samples collected from stressed plants at ST3 and ST4 occupied the furthest distance from samples collected at ST1 and ST6. Samples collected from stressed plants under the first day of each stress (ST2 of drought stress and ST3 of heat stress) and the first day of the stress condition removal (ST5) occupied an intermediate space between samples at ST1/ST6 and ST3/ST4 (Fig 7). Non-stressed samples and stressed samples were separated globally from each other.

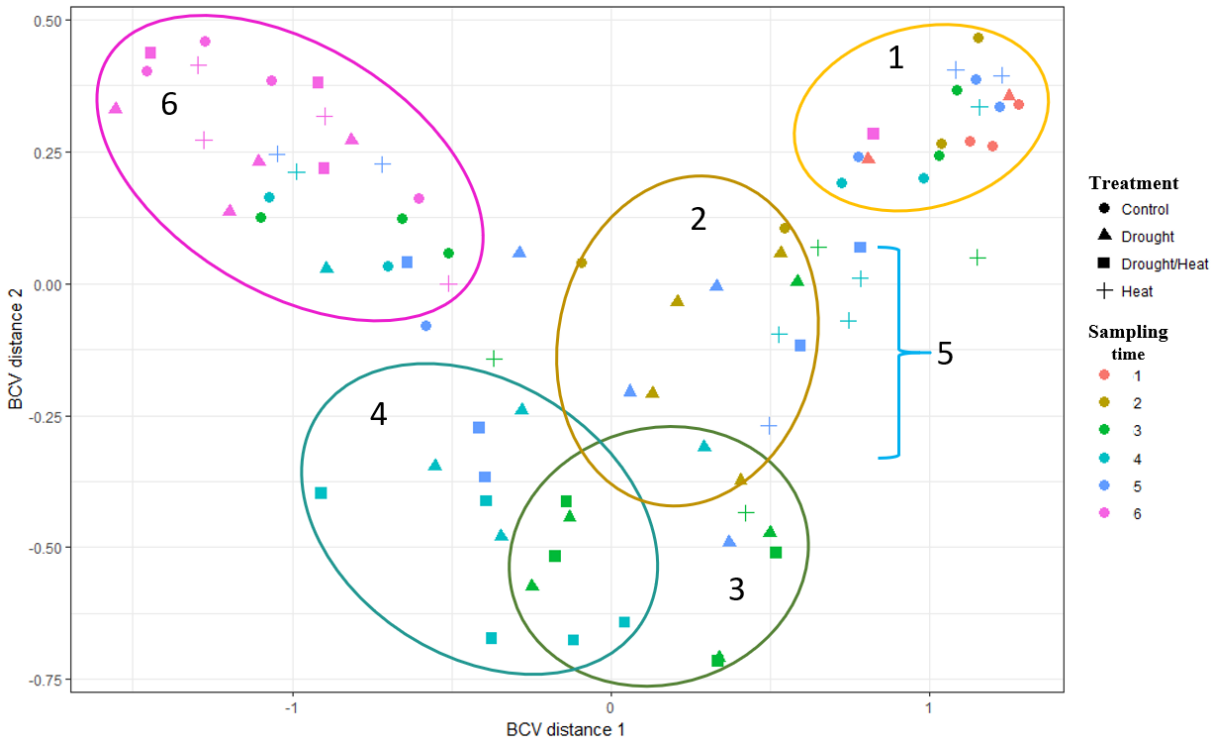

Fig. 7. Effect of drought, heat and drought/heat stress on grapevine transcriptome. The normalised sequencing data was used for multidimensional scaling (MDS) analysis. Four symbols indicate the four treatments, respectively, circle (control), triangle (drought), cross (heat) and square (drought/heat). Six colours indicate the six sampling times. **1**, 1st day plant acclimation to glasshouse; **2**, 1st day of drought treatment; **3**, 11th day of drought treatment and 1st day of heat treatment; **4**, 12th day of drought stress and 2nd day of heat treatment; **5**, Day of stress removal; **6**, 16 days after removal of stress treatments. The separation distance is based on log2 fold change. The more similar expression pattern shows the closer distance.

3.4 Differential Expressed Genes (DEGs) Analysis under Drought and Heat Stresses

To interpret and analyse the RNA-seq data, the differential expression of transcripts was examined between treatments and control (drought vs. control, heat vs. control, drought/heat vs. control). The differentially up-regulated and down-regulated genes were identified for the drought, heat and drought/heat treatments, respectively. More specifically, up-regulated genes were identified 169 under drought stress, 85 under heat stress and 1218 under drought/heat stress; Down-regulated genes were identified 78 under drought stress, 72 under heat stress and 1427 under drought/heat stress (Table 2). Differential expression analysis revealed that the majority of up-regulated and down-regulated genes were identified in the drought/heat treatment (Table 2).

Table 2. **Number of up-regulated and down-regulated differentially expressed genes (DEGs, adjusted P-value<0.01) under drought, heat and drought/heat stress at different sampling times.**

Regulation	Treatment	Sampling times						Total
		1	2	3	4	5	6	
Up-regulated	Drought	0	23	110	36	0	0	169
	Heat	0	0	3	81	1	0	85
	Drought/heat	0	23	236	882	75	2	1218
Down-regulated	Drought	0	37	11	30	0	0	78
	Heat	0	0	2	69	1	0	72
	Drought/heat	0	37	83	1236	71	0	1427

Under drought stress, the number of up-regulated genes increased from 23 at ST2 to 110 at ST3 and then dropped to 36 at ST4 (Table 2, Fig. 8A). Conversely, the number of down-regulated genes decreased from 37 at ST2 to 11 at ST3 and then raised to 30 at ST4 (Table 2). No DEGs were detected on the day of stress removal (ST5) (Table 2).

Under heat condition, the majority of DEGs were enriched at ST4 (Table 2, Fig. 9A). The number of up-regulated DEGs varied from 3 at ST3 to 81 at ST4 whereas the number of down-regulated DEGs varied from 23 at ST3 to 69 at ST4 (Table 2). At ST5 (Day of stress removal), only one up-regulated gene and one down-regulated gene were obtained respectively (Table 2).

In terms of drought/heat treatment, the up-regulated and down-regulated genes both showed a dramatic increase in number (Table 2, Fig. 10). The number of up-regulated DEGs increased from 236 at ST3 to 882 at ST4 while the number of down-regulated DEGs went up from 83 at ST3 to 1236 at ST4 (Table 2). At ST5, 75 up-regulated genes and 71 down-regulated genes were expressed differentially (Table 2). At ST6, there were still two up-regulated DEGs in drought/heat-treated plants (Table 2).

Furthermore, the expression patterns of DEGs were analysed using heat maps to display the expression change and tendency. The heat maps revealed that most DEGs only expressed at one sampling time (Fig. 8B, 9B, 10B). Only a small number of DEGs were observed to express in continuous sampling times, which are analysed with the subsequent result.

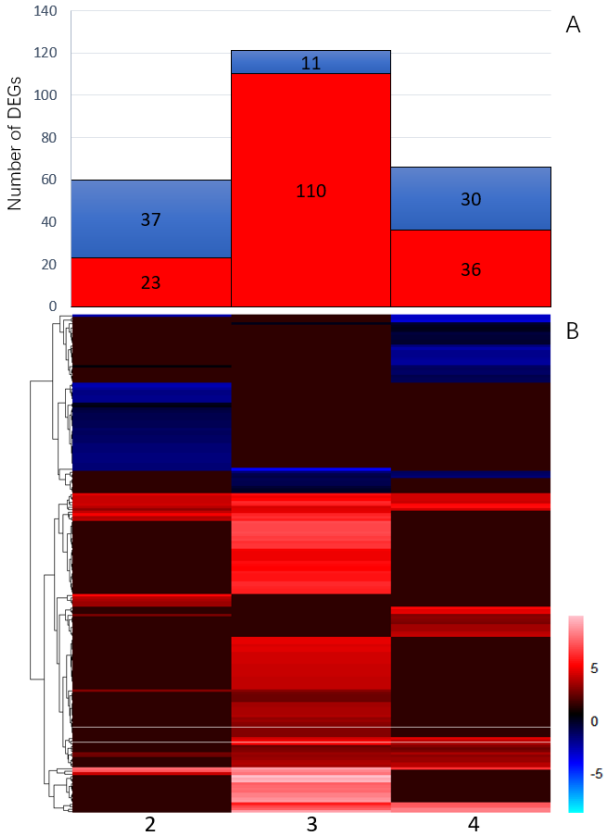

Fig. 8. Differentially expressed genes (DEGs) in drought treatment. (A) Number of up-regulated and down-regulated DEGs at each sampling time. The red colour represents up-regulated DEGs and blue colour represents down-regulated DEGs. (B) Heat map analysis of gene expression based on the log ration fold change (LogFC) data. Each column represents a sampling time, no column means that no DEGs were identified at that sampling time. **2**, 1st day of drought treatment; **3**, 11th day of drought stress and 1st day of heat treatment; **4**, 12th day of drought stress and 2nd day of heat treatment.

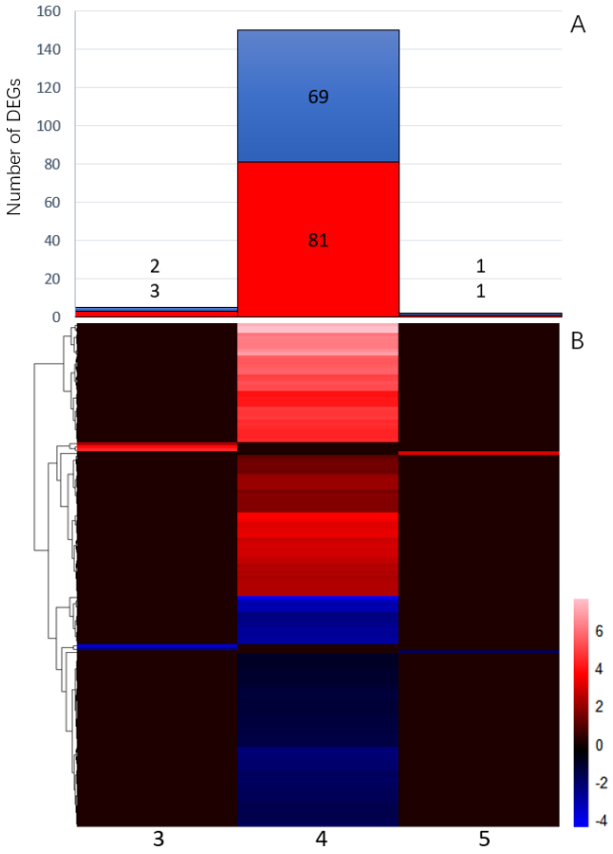

Fig. 9. Differentially expressed genes (DEGs) in heat treatment. The red colour represents up-regulated genes and blue colour represents down-regulated genes. (A) Number of up-regulated and down-regulated DEGs at each sampling time. The red colour represents up-regulated DEGs and blue colour represents down-regulated DEGs. (B) Heat map analysis of gene expression based on the log ration fold change (LogFC) data. Each column represents a sampling time, no column means that no DEGs were identified at that sampling time. **3**, 11th day of drought stress and 1st day of heat treatment; **4**, 12th day of drought stress and 2nd day of heat treatment; **5**, Day of stress removal.

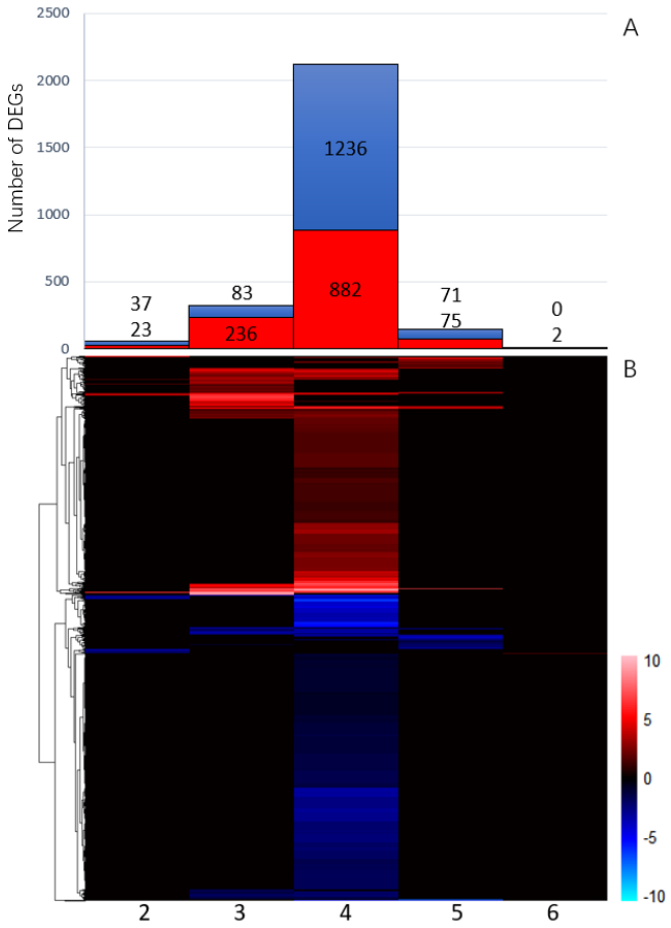

Fig. 10. Differentially expressed genes (DEGs) in the combined drought and heat treatment. (A) Number of up-regulated and down-regulated DEGs at each sampling time. The red colour represents up-regulated DEGs and blue colour represents down-regulated DEGs. (B) Heat map analysis of gene expression based on the log ration fold change (LogFC) data. Each column represents a sampling time, no column means that no DEGs were identified at that sampling time. **2**, 1st day of drought treatment; **3**, 11th day of drought stress and 1st day of heat treatment; **4**, 12th day of drought stress and 2nd day of heat treatment; **5**, Day of stress removal; **6**, 16 days after removal of stress treatments.

3.5 Common Genes during Drought and Heat Treatment

To identify genes associated with each treatment, the common and specific DEGs were detected across three treatments. As can be seen from Fig. 11, drought or heat treatment shared the most DEGs with the combined stress. Additionally, many other genes only involved in response to the combined stress.

At ST3, three common up-regulated DEGs were shared among all treatments (Fig. 11A), respectively, VIT_15s0048g02870, VIT_16s0050g02680 and VIT_18s0001g04800 (Supplementary Table S1).

At ST4, three common up-regulated DEGs and four common down-regulated DEGs were found among all treatment (Fig. 11B), and the annotations are described in Supplementary Table S1. Moreover, six up-regulated genes and three down-regulated genes were differentially expressed only due to drought stress (Fig. 11B). Five up-regulated genes and 22 down-regulated genes were differentially expressed only due to heat stress (Fig. 11B).

At ST5 and ST6, there were no common DEGs among all treatment (Fig. 11C, 11D). At ST5, the heat-treated plants expressed differentially one up-regulated gene and one down-regulated gene (Fig. 11C). These two genes were also identified in the drought/heat treatment as well (Fig. 11C). At ST6, there were only two genes expressing differentially in the drought/heat treatment (Fig. 11D).

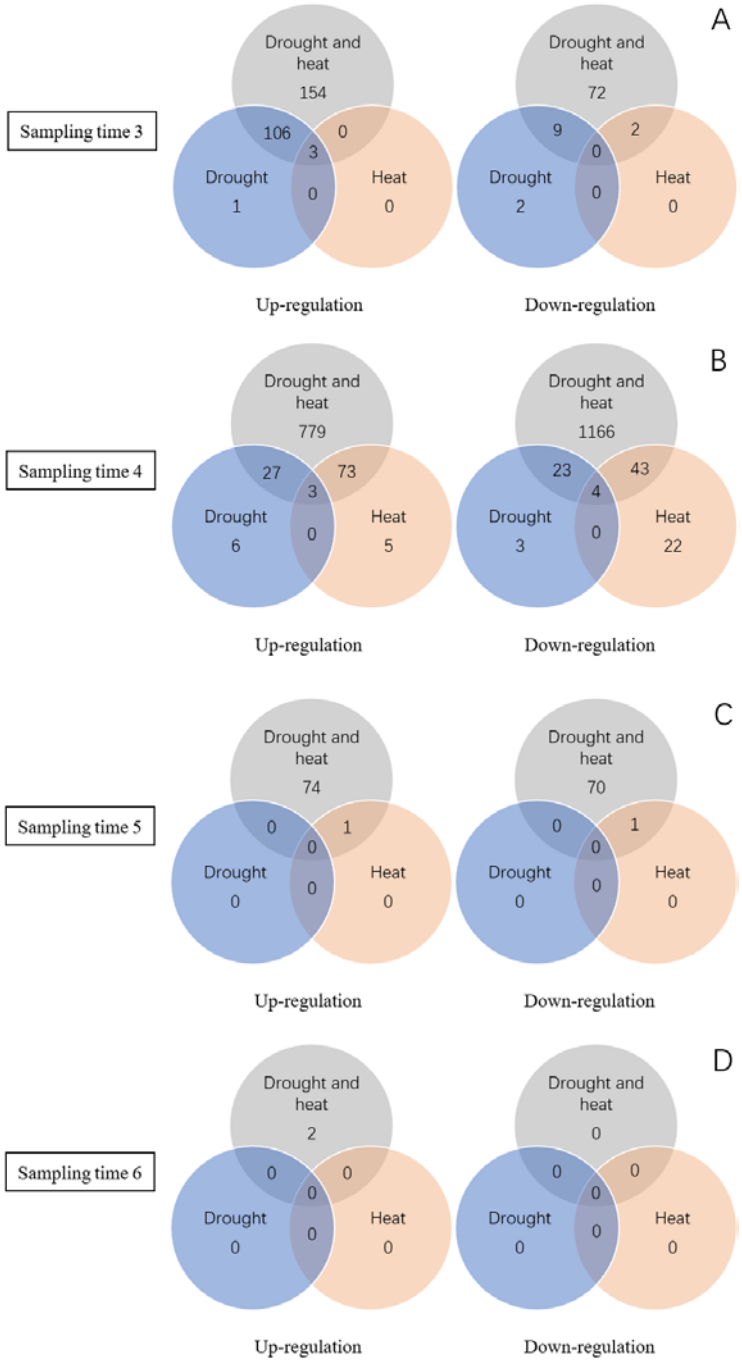

Fig. 11. Venn diagram of up-regulated (left) and down-regulated (right) DEGs from drought, heat and drought/heat at each sampling time. The number represents the common and specific DEGs among three treatments at each sampling time. (A) Sampling time 3, (B) Sampling time 4, (C) Sampling time 5 and (D) Sampling time 6.

To explore how many genes were expressed differentially more than one sampling time in each treatment, the Venn diagram was also used to show the common and specific genes between sampling times.

Under drought stress, 10 common up-regulated DEGs were found over the whole drought treatment (Fig. 12A) and the annotations are described in Supplementary Table S2. However, no common down-regulated gene was being expressed. One down-regulated gene was shared between ST2 and ST3, and 4 down-regulated genes were shared between ST3 and ST4 (Fig. 12A).

Under drought/heat stress, 18 common up-regulated genes and five common down-regulated genes were detected from ST3 to ST5 (Fig. 12C) and the annotations are described in Supplementary Table S3. Additionally, most overlapped genes were expressed differentially between ST3 and ST4, including 150 up-regulated and 68 down-regulated genes. (Fig. 12C). Surprisingly, there were no common DEGs in heat treatment (Fig. 12B).

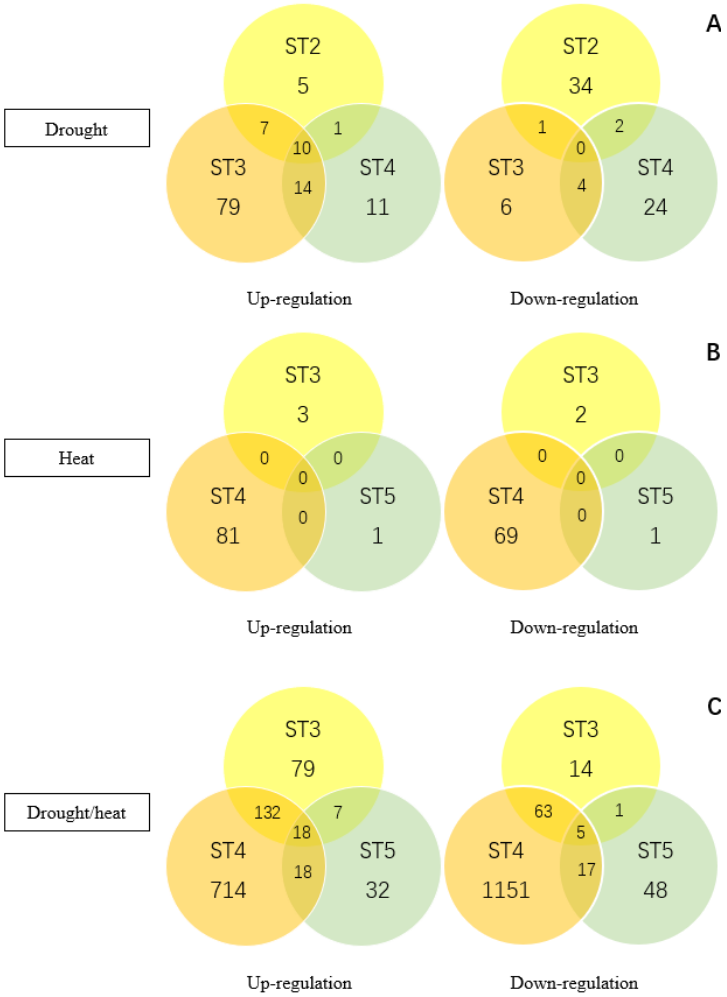

Fig. 12. Venn diagram of up-regulated (left) and down-regulated (right) DEGs in drought, heat, drought/heat treatments over sampling times. The number represents the common and specific DEGs among different sampling times. ST2, 1st day of drought treatment; ST3, 11th day of drought stress and 1st day of heat treatment; ST4, 12th day of drought stress and 2nd day of heat treatment; ST5, Day of stress removal. (A) Drought treatment, (B) Heat treatment and (C) The combined drought and heat treatment.

3.6 Gene Ontology (GO) Analysis of DEGs

To classify DEGs under drought and heat stresses, GO analysis was performed to obtain the biological functions. GO terms were shown for each treatment in Supplementary Table S4, S5 and S6. A total of 154, 132 and 534 GO terms were identified respectively in drought, heat and drought/heat treatments (Fig. 13). The biological functions of DEGs are classified into three main categories such as cellular component (CC), molecular function (MF) and biological process (BP) (Young *et al.*, 2010). Furthermore, the cluster representative of GO analysis was used to visualize and summarize the correlated GO terms.

In 154 GO terms of drought treatment, the fraction distributions for biological process (103), molecular function (32) and cellular component (19) were 66.88%, 20.78% and 12.34% respectively (Fig. 13A). Cluster representative showed four main aspects in response to drought stress such as immune response, glyoxylate cycle, copper ion transport and regulation of multi-organism process (Fig. 14A). In the immune response, GO terms of “regulation of response to abiotic stimulus”, “response to high light intensity” and “response to cytokinin”, “response to nitrate” were retrieved (Fig. 14A). In the glyoxylate cycle, “glyoxylate metabolism”, “asparagine biosynthesis” and “sulfate reduction” were involved in this process (Fig. 14A). The network visualisation displays a mutual relationship among different stress responses (Supplementary Fig. S1). In the Supplementary Table S4, the most significant GO term was described as “regulation of systemic acquired resistance” (GO:0010112). In terms of molecular function, chitin displayed a significant function in response to drought stress, such as “chitin

binding" (GO:0008061), "chitin metabolic process" (GO:0006030) and "chitinase activity" (GO:0004568).

In 132 GO terms of heat treatment, the fraction distributions for biological process (74), molecular function (44) and cellular component (14) were 56.06%, 33.33% and 10.61% respectively (Fig. 13B). Cluster representative revealed three main aspects such as peptidyl-threonine phosphorylation, response to temperature stimulus and diterpenoid metabolism (Fig. 14B). "Response to temperature stimulus", "response to abiotic stimulus" and "response to high light intensity" are observed in the cluster representative plot (Fig. 14B). Additionally, the network visualisation also highlights nitrate, nitric oxide, nitrogen and reactive oxygen species in the network (Supplementary Fig. S2). In the Supplementary Table S5, as the important cellular components in plants, plastid (GO:0044435, GO:0009536, GO:0009532) and chloroplast (GO:0009507, GO:0044434, GO:0009570, GO:0009941) showed the significant abundances in GO terms.

In 533 GO terms of drought/heat treatment, the fraction distributions for biological process (348), molecular function (119) and cellular component (66) were 65.29%, 23.33% and 12.38% respectively (Fig. 13C). In the Supplementary Table S6, the same GO terms as drought treatment and heat treatment were identified such as "response to abiotic stimulus" (GO:0009628), "response to heat" (GO:0009408). Cluster representative displayed five aspects including purine ribonucleotide metabolism, response to abiotic stimulus, anion transport, carbohydrate catabolism and protein-DNA complex assembly (Fig. 14C). GO terms of

“response to abiotic stimulus”, “response to heat”, “response to cytokinin”, “response to chemical” and “immune response” were detected in response to drought/heat treatment (Fig. 14C). “Ion transport”, “sulfate transport” and “hydrogen transport” were observed in anion transport (Fig. 14C). The network visualisation shows a tight connection among those GO terms (Supplementary Fig. S3).

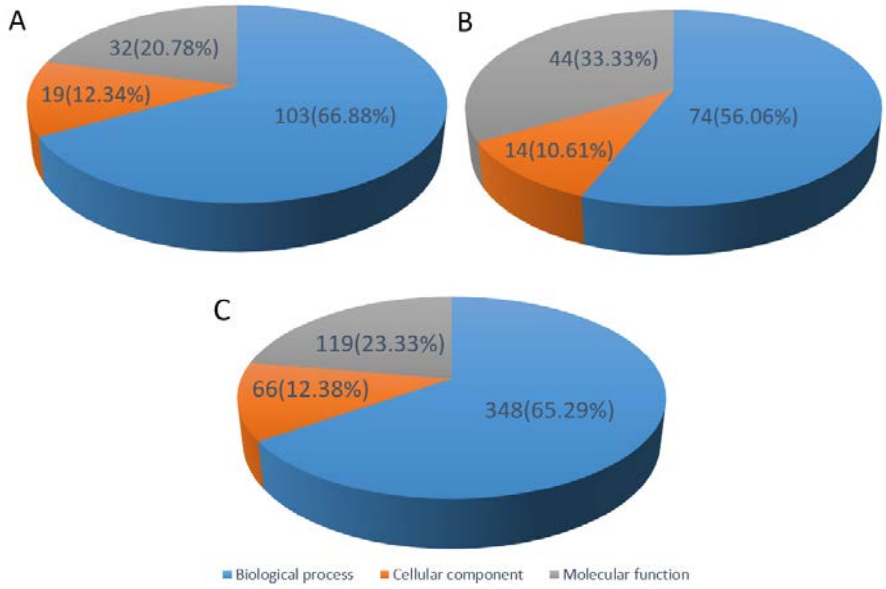

Fig. 13. Percentage distribution of GO terms based on biological process, cellular component and molecular function. (A) 154 GO terms of drought treatment, (B) 132 GO terms of heat treatment, and (C) 534 GO terms of drought/heat treatment.

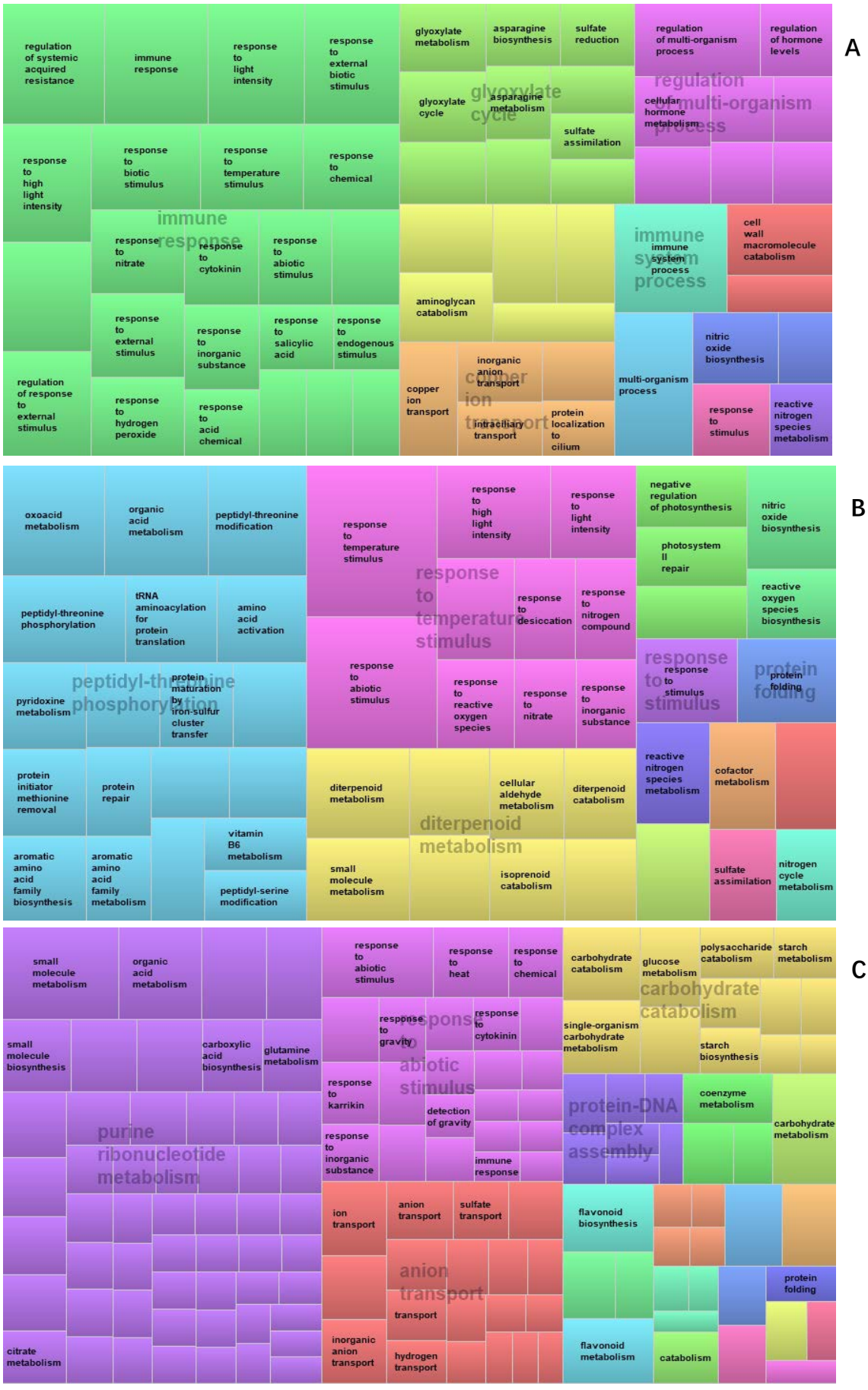

Fig. 14. Cluster representative of GO analysis under stress using REVIGO. Each box is a

single cluster representative. Different representatives are joined into a summarized cluster, visualized with different colours. Boxes with the same colour are clustered by semantic similarity. Box size represents the P-value of GO terms in the Uniprot database. The highly significant GO terms are displayed in boxes. (A) Drought treatment, (B) Heat treatment, and (C) Drought/heat treatment. (http://revigo.irb.hr/)

4. Discussion

4.1 Physiological Performance under Drought and Heat Stress

Drought and heat stresses are the major limiting factors of grapevine production and quality. Winegrowing is practised more often in warmer areas, such as the Mediterranean climate regions, where during the growing season, the midday temperatures can reach 40°C (Banilas *et al.*, 2012). In this study, the air temperature of heat treatment was above 40°C during heat treatment (Fig. 3B). As a supplementary indicator of air temperature, the VPD was also measured (Fig. 3A). The fluctuation change of air temperature can result in the corresponding change of VPD (Zeppel *et al.*, 2012). In order to reflect the stress level of plants during the treatment, the stomatal conductance, stem water potential and leaf temperature were used for analysis and comparison. Firstly, stomatal conductance was widely found in plant leaf to be well correlated with water deficits (Cramer, 2010). In this study, stomatal conductance was also used as an indication of the physiological recovery of stressed plants (Fig.3C). Secondly, stem water potential measurement was suitable for the full expanded leaves to determine the grapevine water status (Choné, 2001; Mirás-Avalos and Intrigliolo, 2017). Thirdly, leaf temperature reflects well the variation of surface temperature in grapevine. Compared with young leaves, the lower leaf temperature of first fully expanded leaves was found in single heat treatment (Fig 6), because the mature leaves have more stomates than young leaves (Rawson and Craven, 1975). Evaporative water of stomate respiration contributed to the reduced leaf temperature.

There is a relationship where heat stress decreased the stem water potential of grapevine leaf (Fig 5) and water loss resulted in the slight rise of leaf temperature in the drought-treated plants (Fig 6). This relationship between water potential and leaf temperature was reported previously (Syvertsen and Levy, 1982). Furthermore, stomatal conductance of heat-treated plants increased obviously at ST3 (1st day of heat treatment) (Fig. 4). During the heat treatment, the single heat-treated plants were still watered. The short-term heat stress causes stomatal opening because the leaf guard cells promote the transpiration rate to control the leaf temperature (Lu *et al.*, 2000). Mott et al. (2010) also suggested that the stomatal opening is relevant to transpiration rate, but the humidity factor is worth being considered. With the reduced water in plants, when the transpiration rate is higher than water uptake rate, stomates closed to diminish water loss (Lu *et al.*, 2000; Liu *et al.*, 2011; Urban *et al.*, 2017).A dramatic decline of stomatal conductance of single heat-treated plants was observed at ST4 (2nd day of heat treatment) (Fig. 4). The continuous high temperature stimulus caused stomatal closure. As a result, leaf temperature of grapevine experienced a significant rise in the heat-treated plants (Fig. 6). Moreover, Merilo et al. (2014) suggested that ion transport proteins involve in stomatal response mechanisms, such as anion channels, K^+ channels and H^+-ATPases. Recently, Nitric Oxide (NO)-induced stomatal closure has been discussed in response to abiotic stress (Yu *et al.*, 2014; Fancy *et al.*, 2017), especially heat stress (Parankusam *et al.*, 2017). After removal of stress treatments (ST5), a quick recovery of water status was observed in stress-treated plants (Fig. 5). That is because the xylem vessels of grapevines are relatively larger than those of other crops and the capacity of water uptake and water transport can benefit from the xylem characteristics of grapevine rootstocks (Serra *et al.*, 2014).

4.2 Combined Drought and Heat Stress Resulted in More DEGs

In this study, the most meaningful design is to add a combined drought and heat treatment. Without sufficient water, a series of biological processes cannot be performed normally. To satisfy the basic demands, photosynthesis is still processing but the photosynthesis rate becomes low due to the decreased respiration rate and deficient water transport (Rollins *et al.*, 2013). Consequently, plant growth is suppressed because plant production is reduced severely. Under single heat stress, plants can utilise water evaporation to reduce leaf temperature (Lu *et al.*, 2000; Urban *et al.*, 2017). Under drought and heat stress, nevertheless, plants do not have sufficient water to reduce leaf temperature. On the one hand plants need to maintain survival; on the other hand, plants attempt to reduce leaf temperature. Thus, some special mechanisms occur to promote the possibility of survival.

In this study, the combined stress imposed a great pressure on water retention in grapevine (Fig 5). As a result, the plants under drought/heat stress produced a large number of functional genes to protect themselves, with approximately 5-fold up-regulated and 10-fold down-regulated DEGs compared to the sum of other single treatments (Table 2). Response to the combined stress, the cluster representative of GO analysis highlights two metabolic pathways: purine ribonucleotide metabolism and carbohydrate catabolism (Fig. 14). Briefly, purine ribonucleotide is the essential building block for RNA and carbohydrate catabolism is a process to yield energy. The purpose of related gene expressions is likely to maintain the fundamental synthesis and growth.

4.3 Cytokinin-activated Signalling Pathway Associated with Drought Stress

Plant hormones play a crucial role in plant growth and development as well as stress response. The function of ABA has been widely discussed as “stress hormone”. Verslues (2016) suggested that cytokinin is also important, involving in a wide range of regulations to enhance stress tolerance. Cytokinin is well known in the cell cycle of shoots and roots. In this study, the plant hormone cytokinin was identified from the immune response in drought treatment based on cluster representative (Fig. 14A). GO terms of “cellular cytokinin-activated signalling pathway” (GO:0009736), “cellular response to cytokinin stimulus” (GO:0071368), “response to cytokinin” (GO:0009735) and “response to cytokinin stimulus” (GO:0071368) highlighted the significance of cytokinin in response to drought stress (Supplementary Table S4). The closed relationship between cytokinin and drought tolerance was reported in *Arabidopsis thaliana* (Huang *et al.*, 2008). As the soil water decreased, the shoot cytokinin concentration declined in tomato (Kudoyarova *et al.*, 2007). With the loss of water in plants, the decline of cytokinin concentration is associated with the stomatal closure (Liu *et al.*, 2013). Additionally, Macková et al. (2013) found that tobacco plants maintained a certain level of bioactive cytokinin under the early stage of drought and heat stress. Cytokinin metabolism was detected to participate in ABA signalling transduction (Zwack and Rashotte, 2015). Recently, some transgenic research provides the evidence to support the function of cytokinin in drought tolerance. Kuppu et al. (2013) showed the improvement of cytokinin biosynthesis in transgenic cotton was effective to enhance the drought tolerance. The stress-induced cytokinin biosynthesis increased drought tolerance in the transgenic rice (Reguera *et al.*, 2013). Pospíšilová et al. (2016) reported the improvement of drought tolerance could be applied in the transgenic barley. In addition, drought

resistance could be exhibited in the change in expression of gene encoding hormone-associated pathways (Peleg *et al.*, 2011; Pospíšilová *et al.*, 2016). Liu et al. (2013) proposed that cytokinin-production could slow down the shoot growth by promoting rhizobacteria to cope with drought stress. From the results of GO analysis, cytokinin may be a crucial plant hormone, involving in drought tolerance in grapevine.

4.4 Plant Ion Transport and Drought Stress Response

Plant ion transport is a basic activity in plant growth and development (Blatt, 2001). Plant ion channel is an essential structure in plant ion transport, such as anion, potassium and hydrogen ion channels in the plasma membrane (Ward et al., 2009). As a basic component, the plant ion channel can participate in various signal transduction pathways in response to stress. GO analyses highlight the function of ion transport in response to drought stress, especially copper ion transport (Fig. 14A), hydrogen transport and anion transport (Fig. 14C). In plants, photosynthesis is a process, where hydrogen ion exchange takes place in the ion channels of chloroplast (Checchetto *et al.*, 2013). In chloroplasts, copper is a key element in chloroplast proteins (Aguirre and Pilon, 2015). Under stress conditions, the necessary ion exchanges are still in progress to maintain plant growth. Apel et al. (2004) reviewed that the abiotic stress can cause an increasing amount of reactive oxygen species (ROS) and oxidative stress can impact the cellular structure. Pottosin et al. (2014) discussed the negative effects of ROS on the ion transport proteins.

Furthermore, Marten et al. (2010) suggested that the anion channels of plasma membrane could involve in regulation of protein phosphorylation. Drought stress affected the expression of ABA-responsive genes through the phosphorylation of binding factors of ABA-responsive element (Cutler et al., 2010). Li et al. (2017) found that the phosphorylation of a WRKY transcription factor affects the expression of drought-responsive genes in cotton. Genes related to ion binding were identified in response to drought by RNA-seq analysis (Müller et al., 2017). However, how the ion transports interact and regulate the stress response process remains largely unknow.

4.5 Nitric Oxide (NO)-mediated Pathway in Response to Heat Stress

NO is a key signalling molecule in response to heat stress (Parankusam *et al.*, 2017). In agreement with the important finding, the significant GO terms of "nitric oxide metabolic process" (GO:0046209), "nitric oxide biosynthetic process" (GO:0006809) and "nitrogen cycle metabolic process" (GO:0071941) were identified in the heat treatment (Supplementary Table S5). Additionally, "response to nitrate" and "response to nitrogen compound" were observed in the cluster representative of response to temperature stimulus in heat treatment (Fig 14B). As a small molecule, NO is an ideal signalling molecule in plant signalling pathway. NO can pass the double layer of cell membranes by simple diffusion (Fancy *et al.*, 2017). In plants, the nitrate uptake is through the plasma membrane of root cells (Crawford, 1995). NADH or xanthine can be used as the catalytic substrate to reduce nitrite to NO (Godber *et al.*, 2000). Nitrate reductase (NR) is an important enzyme to produce the part of NO source by the reduction of nitrite (NO^{2-}) (Rockel *et al.*, 2002). GO terms displayed "nitrate reductase (NADH) activity" (GO:0009703)

and “nitrate reductase (NADPH) activity” (GO:0050464) in the heat treatment (Supplementary Table S5). Further research showed that the catalytic reaction of NR needs a high nitrite concentration and a low oxygen concentration with adequate light condition (Planchet *et al.*, 2005). As antioxidant, NO was shown to react with reactive oxygen species (ROS) generated during heat stress (Parankusam *et al.*, 2017), because NO was reported to activate some antioxidant enzymes (Fancy *et al.*, 2017). The genes coding for “reactive oxygen species biosynthetic process” (GO:1903409) and “response to reactive oxygen species” (GO:0000302) were both found under heat condition (Supplementary Table S5). Thus, GO analysis reveals NO-mediated pathway may be a key pathway of heat stress response in grapevine.

4.6 Other Drought and Heat Tolerance Strategies

In addition to the above discussion, other drought and heat tolerance strategies are suggested in the cluster representative of GO analysis. Under drought stress, glyoxylate cycle is likely to improve drought tolerance in grapevine (Fig. 14A). In this metabolic process, glyoxylate, asparagine and sulfate may be the essential intermediary compounds (Fig. 14A). The up-regulation of asparagine synthetase gene *TaASN1* was induced by salt stress, osmotic stress and ABA in wheat (Wang *et al.*, 2005). The related genes of glyoxylate cycle were identified in rice under abiotic stresses, involving in glucose accumulation (Todaka *et al.*, 2015). Under heat condition, a high correlation of genes encoding peptidyl-threonine phosphorylation was observed (Fig. 14B). In Arabidopsis, Nellaepalli et al. (2011) found that the threonine sites of major light harvesting complex II were phosphorylated under heat stress using immunoblotting. Compared to heat-sensitive sweet maize, the genes of threonine metabolism were up-regulated

in heat-resistant sweet maize under heat condition (Shi *et al.*, 2017). In addition, based on the cluster representative of peptidyl-threonine phosphorylation, “amino acid activation”, “tRNA aminoacylation for protein translation” and “protein repair” imply that this process is likely to repair the cellular damage under heat stress.

In conclusion, the physiological results demonstrated that both drought stress and heat stress contributed mainly to the reduced water status in grapevine. RNA-seq was used to identify three groups of DEGs associated with drought, heat and drought/heat conditions, respectively. Multidimensional scaling (MDS) analysis validated the global difference and similarity of expression pattern. Differential expression analysis revealed that drought/heat stress resulted in a larger number of DEGs than drought stress or heat stress. There were 169, 85 and 1218 up-regulated genes, and 78, 72 and 1427 down-regulated genes, respectively in drought, heat and the combined treatment. Heat map and Venn diagram showed that the majority of genes were expressed differentially only in one certain sampling time. Moreover, a total of 154, 132 and 534 GO terms were identified in drought, heat and drought/heat treatments, respectively. Based on GO terms, “response to abiotic stimulus”, “response to temperature stimulus”, “response to heat” were observed to link with stresses. Further GO analysis suggested that cytokinin-activated signalling pathway, ion transport pathway and Nitric Oxide-mediated pathway play a key role in drought and heat tolerance in grapevine. These results show the complexity of stress response and provide a new insight into the survival purposes of gene expression under drought/heat stress. For further study, qRT-PCR can be used to validate the differential expressed candidate genes, such as those genes involved in suggested pathways. DNA methylation will be investigated to find whether the down-regulated genes are affected by

methylation under stress conditions. Furthermore, the regulatory effect of small RNAs on stress-related gene expression should be considered in the epigenetic levels. The interactive relation between DNA methylation and small RNAs in the context of gene expression in response to stress tolerance will be the subject of future research.

Acknowledgment

I would like to thank my supervisor Carlos M. Rodriguez López and my partners Kiflu Tesfamicael, Pastor Jullian Fabres for collaborating experiment, Na Sai, Konstantinos Bogias and Jimmy Breen for the consultation and support of bioinformatic analysis, and Carlos M. Rodriguez López, Jessica Anne Scott for critical reading of the manuscript. Moreover, I want to thank everyone who helped me in this year, especially all members of Environment Epigenetics and Genetics Group (EEGG).

Reference

Aguirre G, Pilon M. 2015. Copper Delivery to Chloroplast Proteins and its Regulation. Frontiers in plant science **6**, 1250.

Apel K, Hirt H. 2004. Reactive oxygen species: metabolism, oxidative stress, and signal transduction. Annual review of plant biology **55**, 373–399.

Araus JL, Slafer GA. 2011. *Crop stress management and global climate change*. Wallingford, Oxfordshire, UK: CABI.

Bandurska H, Niedziela J, Pietrowska-Borek M, Nuc K, Chadzinikolau T, Radzikowska D. 2017. Regulation of proline biosynthesis and resistance to drought stress in two barley (Hordeum vulgare L.) genotypes of different origin. Plant Physiology and Biochemistry **118**, 427–437.

Banilas G, Korkas E, Englezos V, Nisiotou AA, Hatzopoulos P. 2012. Genome-wide analysis of the heat shock protein 90 gene family in grapevine (*Vitis vinifera* L.). Australian journal of grape and wine research **18**, 29–38.

Carvalho LC, Coito JL, Colaço S, Sangiogo M, Amâncio S. 2015. Heat stress in grapevine: the pros and cons of acclimation. Plant, Cell & Environment **38**, 777–789.

Chaves MM, Zarrouk O, Francisco R, Costa JM, Santos T, Regalado AP, Rodrigues ML, Lopes CM. 2010. Grapevine under deficit irrigation: hints from physiological and molecular data. Annals of Botany **105**, 661–676.

Checchetto V, Teardo E, Carraretto L, Formentin E, Bergantino E, Giacometti GM, Szabo I. 2013. Regulation of photosynthesis by ion channels in cyanobacteria and higher plants. Biophysical Chemistry **182**, 51–57.

Chen S, Li H. 2016. Heat Stress Regulates the Expression of Genes at Transcriptional and Post-Transcriptional Levels, Revealed by RNA-seq in *Brachypodium distachyon*. Frontiers in plant science **7**, 2067.

Choné X. 2001. Stem Water Potential is a Sensitive Indicator of Grapevine Water Status. Annals of Botany **87**, 477–483.

Coolen S, Proietti S, Hickman R, *et al.* 2016. Transcriptome dynamics of Arabidopsis during sequential biotic and abiotic stresses. The Plant Journal: for Cell and Molecular Biology **86**, 249–267.

Cramer GR. 2010. Abiotic stress and plant responses from the whole vine to the genes. Australian journal of grape and wine research **16**, 86–93.

Crawford NM. 1995. Nitrate: nutrient and signal for plant growth. The Plant Cell **7**, 859–868.

Dai A. 2011. Drought under global warming: a review. Wiley Interdisciplinary Reviews: Climate Change **2**, 45–65.

Fancy NN, Bahlmann A-K, Loake GJ. 2017. Nitric oxide function in plant abiotic stress. Plant, Cell & Environment **40**, 462–472.

Fuentes S, De Bei R, Tyerman S. 2013. The Vineyard of The Future: A Fully Instrumented Vineyard for Climate Change Research.

Garnaut R. 2008. *The Garnaut climate change review: Final report*. Cambridge: Cambridge University Press.

Godber BL, Doel JJ, Sapkota GP, Blake DR, Stevens CR, Eisenthal R, Harrison R. 2000. Reduction of nitrite to nitric oxide catalyzed by xanthine oxidoreductase. The Journal of Biological Chemistry **275**, 7757–7763.

Hall A, Jones GV. 2009. Effect of potential atmospheric warming on temperature-based indices describing Australian winegrape growing conditions. Australian journal of grape and wine research **15**, 97–119.

Huang D, Wu W, Abrams SR, Cutler AJ. 2008. The relationship of drought-related gene expression in Arabidopsis thaliana to hormonal and environmental factors. Journal of Experimental Botany **59**, 2991–3007.

Hübner S, Korol AB, Schmid KJ. 2015. RNA-Seq analysis identifies genes associated with differential reproductive success under drought-stress in accessions of wild barley Hordeum spontaneum. BMC Plant Biology **15**, 134.

Kang MS, Banga SS. 2013. Global agriculture and climate change. Journal of Crop Improvement **27**, 667–692.

Khalil-Ur-Rehman M, Sun L, Li C-X, Faheem M, Wang W, Tao J-M. 2017. Comparative RNA-seq based transcriptomic analysis of bud dormancy in grape. BMC Plant Biology **17**, 18.

Kim D, Langmead B, Salzberg SL. 2015. HISAT: a fast spliced aligner with low memory requirements. Nature Methods **12**, 357–360.

Kudoyarova GR, Vysotskaya LB, Cherkozyanova A, Dodd IC. 2007. Effect of partial rootzone drying on the concentration of zeatin-type cytokinins in tomato (Solanum lycopersicum L.) xylem sap and leaves. Journal of Experimental Botany **58**, 161–168.

Kuppu S, Mishra N, Hu R, Sun L, Zhu X, Shen G, Blumwald E, Payton P, Zhang H. 2013. Water-deficit inducible expression of a cytokinin biosynthetic gene IPT improves drought tolerance in cotton. Plos One **8**, e64190.

Lindgreen S. 2012. AdapterRemoval: easy cleaning of next-generation sequencing reads. BMC

Research Notes **5**, 337.

Liu Y, Subhash C, Yan J, Song C, Zhao J, Li J. 2011. Maize leaf temperature responses to drought: Thermal imaging and quantitative trait loci (QTL) mapping. Environmental and experimental botany **71**, 158–165.

Liu F, Xing S, Ma H, Du Z, Ma B. 2013. Cytokinin-producing, plant growth-promoting rhizobacteria that confer resistance to drought stress in Platycladus orientalis container seedlings. Applied Microbiology and Biotechnology **97**, 9155–9164.

Lu Z, Quiñones MA, Zeiger E. 2000. Temperature dependence of guard cell respiration and stomatal conductance co-segregate in an F2 population of Pima cotton. Functional Plant Biology **24**, 457-462.

Lun ATL, Chen Y, Smyth GK. 2016. It's DE-licious: A Recipe for Differential Expression Analyses of RNA-seq Experiments Using Quasi-Likelihood Methods in edgeR. Methods in Molecular Biology **1418**, 391–416.

Macková H, Hronková M, Dobrá J, *et al.* 2013. Enhanced drought and heat stress tolerance of tobacco plants with ectopically enhanced cytokinin oxidase/dehydrogenase gene expression. Journal of Experimental Botany **64**, 2805–2815.

Magalhães AP, Verde N, Reis F, Martins I, Costa D, Lino-Neto T, Castro PH, Tavares RM, Azevedo H. 2015. RNA-Seq and Gene Network Analysis Uncover Activation of an ABA-Dependent Signalosome During the Cork Oak Root Response to Drought. Frontiers in plant science **6**, 1195.

Meggio F, Prinsi B, Negri AS, Simone Di Lorenzo G, Lucchini G, Pitacco A, Failla O, Scienza A, Cocucci M, Espen L. 2014. Biochemical and physiological responses of two

grapevine rootstock genotypes to drought and salt treatments. Australian journal of grape and wine research **20**, 310–323.

Merilo E, Jõesaar I, Brosché M, Kollist H. 2014. To open or to close: species-specific stomatal responses to simultaneously applied opposing environmental factors. The New Phytologist **202**, 499–508.

Mira de Orduña R. 2010. Climate change associated effects on grape and wine quality and production. Food Research International **43**, 1844–1855.

Mirás-Avalos JM, Intrigliolo DS. 2017. Grape Composition under Abiotic Constrains: Water Stress and Salinity. Frontiers in plant science **8**, 851.

Moore AD, Robertson MJ, Routley R. 2011. Evaluation of the water use efficiency of alternative farm practices at a range of spatial and temporal scales: A conceptual framework and a modelling approach. Agricultural systems **104**, 162–174.

Mott KA, Peak D. 2010. Stomatal responses to humidity and temperature in darkness. Plant, Cell & Environment **33**, 1084–1090.

Nellaepalli S, Mekala NR, Zsiros O, Mohanty P, Subramanyam R. 2011. Moderate heat stress induces state transitions in Arabidopsis thaliana. Biochimica et Biophysica Acta **1807**, 1177–1184.

Parankusam S, Adimulam SS, Bhatnagar-Mathur P, Sharma KK. 2017. Nitric oxide (NO) in plant heat stress tolerance: current knowledge and perspectives. Frontiers in plant science **8**, 1582.

Peleg Z, Reguera M, Tumimbang E, Walia H, Blumwald E. 2011. Cytokinin-mediated source/sink modifications improve drought tolerance and increase grain yield in rice under

water-stress. Plant Biotechnology Journal **9**, 747–758.

Phogat V, Skewes MA, McCarthy MG, Cox JW, Šimůnek J, Petrie PR. 2017. Evaluation of crop coefficients, water productivity, and water balance components for wine grapes irrigated at different deficit levels by a sub-surface drip. Agricultural Water Management **180**, 22–34.

Planchet E, Jagadis Gupta K, Sonoda M, Kaiser WM. 2005. Nitric oxide emission from tobacco leaves and cell suspensions: rate limiting factors and evidence for the involvement of mitochondrial electron transport. The Plant Journal: for Cell and Molecular Biology **41**, 732–743.

Pospíšilová H, Jiskrová E, Vojta P, *et al.* 2016. Transgenic barley overexpressing a cytokinin dehydrogenase gene shows greater tolerance to drought stress. New biotechnology **33**, 692–705.

Pottosin I, Velarde-Buendía AM, Bose J, Zepeda-Jazo I, Shabala S, Dobrovinskaya O. 2014. Cross-talk between reactive oxygen species and polyamines in regulation of ion transport across the plasma membrane: implications for plant adaptive responses. Journal of Experimental Botany **65**, 1271–1283.

Rawson H, Craven C. 1975. Stomatal development during leaf expansion in tobacco and sunflower. Australian journal of botany **23**, 253.

Reguera M, Peleg Z, Abdel-Tawab YM, Tumimbang EB, Delatorre CA, Blumwald E. 2013. Stress-induced cytokinin synthesis increases drought tolerance through the coordinated regulation of carbon and nitrogen assimilation in rice. Plant Physiology **163**, 1609–1622.

Robinson MD, McCarthy DJ, Smyth GK. 2010. edgeR: a Bioconductor package for differential expression analysis of digital gene expression data. Bioinformatics **26**, 139–140.

Rockel P, Strube F, Rockel A, Wildt J, Kaiser WM. 2002. Regulation of nitric oxide (NO) production by plant nitrate reductase in vivo and in vitro. Journal of Experimental Botany **53**, 103–110.

Rollins JA, Habte E, Templer SE, Colby T, Schmidt J, von Korff M. 2013. Leaf proteome alterations in the context of physiological and morphological responses to drought and heat stress in barley (Hordeum vulgare L.). Journal of Experimental Botany **64**, 3201–3212.

Ben Salem-Fnayou A, Bouamama B, Ghorbel A, Mliki A. 2011. Investigations on the leaf anatomy and ultrastructure of grapevine (*Vitis vinifera*) under heat stress. Microscopy Research and Technique **74**, 756–762.

Serra I, Strever A, Myburgh PA, Deloire A. 2014. Review: the interaction between rootstocks and cultivars (*Vitis vinifera* L.) to enhance drought tolerance in grapevine. Australian journal of grape and wine research **20**, 1–14.

Shi J, Yan B, Lou X, Ma H, Ruan S. 2017. Comparative transcriptome analysis reveals the transcriptional alterations in heat-resistant and heat-sensitive sweet maize (Zea mays L.) varieties under heat stress. BMC Plant Biology **17**, 26.

Soar CJ, Sadras VO, Petrie PR. 2008. Climate drivers of red wine quality in four contrasting Australian wine regions. Australian journal of grape and wine research **14**, 78–90.

Soosay C, Andrew F. 2011. Using sustainable value chain analysis as a catalyst for co-innovation in regional development: a case study of South Australian wine from the Riverland. Int. J. of Innovation and Regional Development **3**, 126–140.

Sun J, Ren L, Cheng Y, Gao J, Dong B, Chen S, Chen F, Jiang J. 2014. Identification of differentially expressed genes in Chrysanthemum nankingense (Asteraceae) under heat stress

by RNA Seq. Gene **552**, 59–66.

Supek F, Bošnjak M, Škunca N, Šmuc T. 2011. REVIGO summarizes and visualizes long lists of gene ontology terms. Plos One **6**, e21800.

Syvertsen JP, Levy Y. 1982. Diurnal changes in citrus leaf thickness, leaf water potential and leaf to air temperature difference. Journal of experimental botany **33**, 783–789.

Thatcher SR, Danilevskaya ON, Meng X, Beatty M, Zastrow-Hayes G, Harris C, Van Allen B, Habben J, Li B. 2016. Genome-Wide Analysis of Alternative Splicing during Development and Drought Stress in Maize. Plant Physiology **170**, 586–599.

Todaka D, Shinozaki K, Yamaguchi-Shinozaki K. 2015. Recent advances in the dissection of drought-stress regulatory networks and strategies for development of drought-tolerant transgenic rice plants. Frontiers in plant science **6**, 84.

Urban J, Ingwers MW, McGuire MA, Teskey RO. 2017. Increase in leaf temperature opens stomata and decouples net photosynthesis from stomatal conductance in Pinus taeda and Populus deltoides x nigra. Journal of Experimental Botany **68**, 1757–1767.

Verslues PE. 2016. ABA and cytokinins: challenge and opportunity for plant stress research. Plant Molecular Biology **91**, 629–640.

Wang L, Feng Z, Wang X, Wang X, Zhang X. 2010. DEGseq: an R package for identifying differentially expressed genes from RNA-seq data. Bioinformatics **26**, 136–138.

Wang H, Liu D, Sun J, Zhang A. 2005. Asparagine synthetase gene TaASN1 from wheat is up-regulated by salt stress, osmotic stress and ABA. Journal of Plant Physiology **162**, 81–89.

Webb LB, Whetton PH, Barlow EWR. 2007. Modelled impact of future climate change on the phenology of winegrapes in Australia. Australian journal of grape and wine research **13**,

165–175.

Wu L, Taohua Z, Gui W, Xu L, Li J, Ding Y. 2015. Five pectinase gene expressions highly responding to heat stress in rice floral organs revealed by RNA-seq analysis. Biochemical and Biophysical Research Communications **463**, 407–413.

Young MD, Wakefield MJ, Smyth GK, Oshlack A. 2010. Gene ontology analysis for RNA-seq: accounting for selection bias. Genome Biology **11**, R14.

Yu M, Lamattina L, Spoel SH, Loake GJ. 2014. Nitric oxide function in plant biology: a redox cue in deconvolution. The New Phytologist **202**, 1142–1156.

Zeppel MJB, Lewis JD, Chaszar B, Smith RA, Medlyn BE, Huxman TE, Tissue DT. 2012. Nocturnal stomatal conductance responses to rising [CO2], temperature and drought. The New Phytologist **193**, 929–938.

Zwack PJ, Rashotte AM. 2015. Interactions between cytokinin signalling and abiotic stress responses. Journal of Experimental Botany **66**, 4863–4871.

Appendix: Supplementary materials

Supplementary Table S1. GO annotation of overlapped genes among drought, heat and drought/heat treatment at ST3, ST4. The biological functions of DEGs are classified into three main categories such as cellular component (CC), molecular function (MF) and biological process (BP).

Regulation	Sampling time	ensembl_gene_id	GO id	Annotation	Ontology
Up-regulated	3	VIT_15s0048g02870	GO:0043565	sequence-specific DNA binding	MF
			GO:0005634	nucleus	CC
			GO:0006355	regulation of transcription, DNA-templated	BP
			GO:0003677	DNA binding	MF
			GO:0003700	transcription factor activity, sequence-specific DNA binding	MF
		VIT_16s0050g02680	GO:0006470	protein dephosphorylation	BP
			GO:0004722	protein serine/threonine phosphatase activity	MF
			GO:0003824	catalytic activity	MF
		VIT_18s0001g04800	GO:0046916	cellular transition metal ion homeostasis	BP
			GO:0030001	metal ion transport	BP
			GO:0046914	transition metal ion binding	MF
			GO:0046872	metal ion binding	MF
			GO:0005737	cytoplasm	CC
	4	VIT_11s0016g04960	GO:0006520	cellular amino acid metabolic process	BP
			GO:0006807	nitrogen compound metabolic process	BP
			GO:0008152	metabolic process	BP
			GO:0016855	racemase and epimerase activity, acting on amino acids and derivatives	MF
			GO:0036361	racemase activity, acting on amino acids and derivatives	MF
		VIT_14s0171g00360			
		VIT_15s0046g01560	GO:0006457	protein folding	BP
			GO:0051087	chaperone binding	MF
			GO:0009506	plasmodesma	CC
			GO:0009266	response to temperature stimulus	BP
			GO:0043207	response to external biotic stimulus	BP
Down-regulated	4	VIT_01s0010g03870	GO:0016021	integral component of membrane	CC
			GO:0016020	membrane	CC
		VIT_02s0025g02960	GO:0055114	oxidation-reduction process	BP
			GO:0046872	metal ion binding	MF
			GO:0016491	oxidoreductase activity	MF
		VIT_18s0001g04910	GO:0008272	sulfate transport	BP
			GO:0015116	sulfate transmembrane transporter activity	MF

			GO:0008271	secondary active sulfate transmembrane transporter activity	MF
			GO:1902358	sulfate transmembrane transport	BP
			GO:0005886	plasma membrane	CC
			GO:0016021	integral component of membrane	CC
			GO:0055085	transmembrane transport	BP
			GO:0016020	membrane	CC
			GO:0005887	integral component of plasma membrane	CC
			GO:0006810	transport	BP
		VIT_18s0001g14010	GO:0016310	phosphorylation	BP
			GO:0000103	sulfate assimilation	BP
			GO:0004781	sulfate adenylyltransferase (ATP) activity	MF
			GO:0004020	adenylylsulfate kinase activity	MF

Supplementary Table S2. GO annotation of 10 overlapped up-regulated genes among sampling times in drought treatment. The biological functions of DEGs are classified into three main categories such as cellular component (CC), molecular function (MF) and biological process (BP).

Regulation	ensembl_gene_id	GO id	Annotation	Ontology
Up-regulated	VIT_02s0025g00240	GO:0008610	lipid biosynthetic process	BP
		GO:0005506	iron ion binding	MF
		GO:0016021	integral component of membrane	CC
		GO:0016020	membrane	CC
		GO:0055114	oxidation-reduction process	BP
		GO:0016491	oxidoreductase activity	MF
Up-regulated	VIT_03s0063g01790			
Up-regulated	VIT_04s0023g02480	GO:0009737	response to abscisic acid	BP
		GO:0006950	response to stress	BP
		GO:0005829	cytosol	CC
		GO:0009414	response to water deprivation	BP
		GO:0009415	response to water	BP
		GO:0009631	cold acclimation	BP
Up-regulated	VIT_05s0029g00480	GO:0016747	transferase activity, transferring acyl groups other than amino-acyl groups	MF
Up-regulated	VIT_12s0059g00490			
Up-regulated	VIT_14s0083g01140	GO:0016021	integral component of membrane	CC
		GO:0016020	membrane	CC
Up-regulated	VIT_14s0108g00450			
Up-regulated	VIT_14s0171g00360			
Up-regulated	VIT_15s0048g02870	GO:0043565	sequence-specific DNA binding	MF
		GO:0005634	nucleus	CC
		GO:0006355	regulation of transcription, DNA-templated	BP
		GO:0003677	DNA binding	MF
		GO:0003700	transcription factor activity, sequence-specific DNA binding	MF
Up-regulated	VIT_16s0050g02680	GO:0006470	protein dephosphorylation	BP
		GO:0004722	protein serine/threonine phosphatase activity	MF
		GO:0003824	catalytic activity	MF

Supplementary Table S3. GO annotation of overlapped 18 up-regulated and 5 down-regulated genes among sampling times in drought/heat treatment. The biological functions of DEGs are classified into three main categories such as cellular component (CC), molecular function (MF) and biological process (BP).

Regulation	ensembl_gene_id	GO id	Annotation	Ontology
Up-regulated	VIT_02s0025g00230			
Up-regulated	VIT_03s0088g00320	GO:0016021	integral component of membrane	CC
		GO:0016020	membrane	CC
Up-regulated	VIT_05s0020g03330	GO:0005524	ATP binding	MF
		GO:0000166	nucleotide binding	MF
		GO:0009408	response to heat	BP
		GO:0009644	response to high light intensity	BP
		GO:0042542	response to hydrogen peroxide	BP
Up-regulated	VIT_06s0004g05770			
Up-regulated	VIT_08s0007g04000			
Up-regulated	VIT_08s0040g03150	GO:0042744	hydrogen peroxide catabolic process	BP
		GO:0000302	response to reactive oxygen species	BP
		GO:0016688	L-ascorbate peroxidase activity	MF
		GO:0004130	cytochrome-c peroxidase activity	MF
		GO:0034599	cellular response to oxidative stress	BP
		GO:0009507	chloroplast	CC
		GO:0098869	cellular oxidant detoxification	BP
		GO:0006979	response to oxidative stress	BP
		GO:0020037	heme binding	MF
		GO:0004601	peroxidase activity	MF
		GO:0055114	oxidation-reduction process	BP
Up-regulated	VIT_09s0002g06790	GO:0009408	response to heat	BP
		GO:0009644	response to high light intensity	BP
		GO:0042542	response to hydrogen peroxide	BP
Up-regulated	VIT_11s0016g03170	GO:0016310	phosphorylation	BP
		GO:0000160	phosphorelay signal transduction system	BP
		GO:0043424	protein histidine kinase binding	MF
		GO:0009927	histidine phosphotransfer kinase activity	MF
		GO:0004871	signal transducer activity	MF
		GO:0009736	cytokinin-activated signaling pathway	BP
		GO:0005737	cytoplasm	CC
		GO:0005634	nucleus	CC

Up-regulated	VIT_11s0016g03180	GO:0006470	protein dephosphorylation	BP
		GO:0043169	cation binding	MF
		GO:0004722	protein serine/threonine phosphatase activity	MF
		GO:0004721	phosphoprotein phosphatase activity	MF
		GO:0016787	hydrolase activity	MF
		GO:0046872	metal ion binding	MF
		GO:0003824	catalytic activity	MF
Up-regulated	VIT_13s0019g02930			
Up-regulated	VIT_13s0019g03000			
Up-regulated	VIT_14s0108g00590	GO:0010304	PSII associated light-harvesting complex II catabolic process	BP
		GO:0010027	thylakoid membrane organization	BP
		GO:0004222	metalloendopeptidase activity	MF
		GO:0006508	proteolysis	BP
		GO:0009941	chloroplast envelope	CC
		GO:0009535	chloroplast thylakoid membrane	CC
		GO:0005524	ATP binding	MF
		GO:0000166	nucleotide binding	MF
		GO:0016020	membrane	CC
		GO:0008237	metallopeptidase activity	MF
		GO:0004176	ATP-dependent peptidase activity	MF
		GO:0010205	photoinhibition	BP
		GO:0010206	photosystem II repair	BP
Up-regulated	VIT_14s0108g01500	GO:0016485	protein processing	BP
		GO:0019538	protein metabolic process	BP
		GO:0009408	response to heat	BP
		GO:0005737	cytoplasm	CC
		GO:0005524	ATP binding	MF
		GO:0000166	nucleotide binding	MF
		GO:0009507	chloroplast	CC
Up-regulated	VIT_14s0171g00360			
Up-regulated	VIT_15s0046g01560	GO:0006457	protein folding	BP
		GO:0051087	chaperone binding	MF
		GO:0009506	plasmodesma	CC
		GO:0009266	response to temperature stimulus	BP
		GO:0043207	response to external biotic stimulus	BP
Up-regulated	VIT_16s0050g02680	GO:0006470	protein dephosphorylation	BP
		GO:0004722	protein serine/threonine phosphatase activity	MF
		GO:0003824	catalytic activity	MF
Up-regulated	VIT_16s0098g01060	GO:0009408	response to heat	BP
		GO:0009644	response to high light intensity	BP
		GO:0042542	response to hydrogen peroxide	BP

		GO:0043621	protein self-association	MF
		GO:0006355	regulation of transcription, DNA-templated	BP
		GO:0009416	response to light stimulus	BP
		GO:0009658	chloroplast organization	BP
		GO:0000427	plastid-encoded plastid RNA polymerase complex	CC
		GO:0042644	chloroplast nucleoid	CC
		GO:0101031	chaperone complex	CC
Up-regulated	VIT_18s0001g02690			
Down-regulated	VIT_03s0063g02620	GO:0005634	nucleus	CC
		GO:0003677	DNA binding	MF
Down-regulated	VIT_05s0049g01550	GO:0016021	integral component of membrane	CC
		GO:0016020	membrane	CC
		GO:0006810	transport	BP
		GO:0005215	transporter activity	MF
Down-regulated	VIT_07s0031g01710	GO:0043565	sequence-specific DNA binding	MF
		GO:0006355	regulation of transcription, DNA-templated	BP
		GO:0003700	transcription factor activity, sequence-specific DNA binding	MF
Down-regulated	VIT_08s0058g00470			
Down-regulated	VIT_11s0016g04270			

Supplementary Table S4. 154 GO terms identified from DEGs of drought treatment. The biological functions of DEGs are classified into three main categories such as cellular component (CC), molecular function (MF) and biological process (BP). DE means the number of DEGs in the GO term. N means the number of non-differentially expressed genes in the GO term from genome database. The list is sorted by P-value.

GO id	Annotation	Type	P-value	DE	N
GO:0010112	regulation of systemic acquired resistance	BP	2.38E-05	3	9
GO:0045087	innate immune response	BP	2.75E-05	5	53
GO:0006955	immune response	BP	3.01E-05	5	54
GO:0002376	immune system process	BP	3.92E-05	5	57
GO:0009814	defense response, incompatible interaction	BP	5.22E-05	4	31
GO:0009642	response to light intensity	BP	5.93E-05	4	32
GO:0043207	response to external biotic stimulus	BP	6.79E-05	7	150
GO:0051704	multi-organism process	BP	7.90E-05	10	331
GO:0009627	systemic acquired resistance	BP	7.94E-05	3	13
GO:0009644	response to high light intensity	BP	1.25E-04	3	15
GO:0002831	regulation of response to biotic stimulus	BP	2.61E-04	3	19
GO:0071368	cellular response to cytokinin stimulus	BP	2.61E-04	3	19
GO:0009736	cytokinin-activated signaling pathway	BP	2.61E-04	3	19
GO:0032101	regulation of response to external stimulus	BP	3.06E-04	3	20
GO:0051707	response to other organism	BP	3.74E-04	6	141
GO:0043900	regulation of multi-organism process	BP	4.09E-04	3	22
GO:0009607	response to biotic stimulus	BP	4.25E-04	7	202
GO:0030151	molybdenum ion binding	MF	4.37E-04	2	5
GO:0045088	regulation of innate immune response	BP	6.02E-04	3	25
GO:0050776	regulation of immune response	BP	6.02E-04	3	25
GO:0009266	response to temperature stimulus	BP	6.70E-04	5	104
GO:0002682	regulation of immune system process	BP	7.59E-04	3	27
GO:0098542	defense response to other organism	BP	1.10E-03	5	116
GO:0042221	response to chemical	BP	1.13E-03	16	1006
GO:0010167	response to nitrate	BP	1.55E-03	2	9
GO:0005375	copper ion transmembrane transporter activity	MF	1.55E-03	2	9
GO:0009605	response to external stimulus	BP	1.58E-03	7	253
GO:0016998	cell wall macromolecule catabolic process	BP	1.77E-03	3	36
GO:0042542	response to hydrogen peroxide	BP	1.92E-03	2	10
GO:0035434	copper ion transmembrane transport	BP	2.34E-03	2	11
GO:0009927	histidine phosphotransfer kinase activity	MF	2.34E-03	2	11
GO:0009408	response to heat	BP	2.41E-03	3	40
GO:0009735	response to cytokinin	BP	2.77E-03	3	42

GO:0009628	response to abiotic stimulus	BP	2.89E-03	9	441
GO:0043424	protein histidine kinase binding	MF	3.29E-03	2	13
GO:0031226	intrinsic component of plasma membrane	CC	3.66E-03	7	294
GO:0006825	copper ion transport	BP	3.82E-03	2	14
GO:0008061	chitin binding	MF	4.81E-03	3	51
GO:0006026	aminoglycan catabolic process	BP	4.81E-03	3	51
GO:0006030	chitin metabolic process	BP	4.81E-03	3	51
GO:0046348	amino sugar catabolic process	BP	4.81E-03	3	51
GO:1901071	glucosamine-containing compound metabolic process	BP	4.81E-03	3	51
GO:1901072	glucosamine-containing compound catabolic process	BP	4.81E-03	3	51
GO:0006032	chitin catabolic process	BP	4.81E-03	3	51
GO:0004568	chitinase activity	MF	4.81E-03	3	51
GO:1901700	response to oxygen-containing compound	BP	4.90E-03	8	392
GO:0010035	response to inorganic substance	BP	5.32E-03	5	167
GO:0006022	aminoglycan metabolic process	BP	5.35E-03	3	53
GO:0055044	symplast	CC	6.62E-03	5	176
GO:0009506	plasmodesma	CC	6.62E-03	5	176
GO:0033759	flavone synthase activity	MF	6.68E-03	1	1
GO:0046487	glyoxylate metabolic process	BP	6.68E-03	1	1
GO:0006097	glyoxylate cycle	BP	6.68E-03	1	1
GO:0004474	malate synthase activity	MF	6.68E-03	1	1
GO:0046209	nitric oxide metabolic process	BP	6.68E-03	1	1
GO:0006809	nitric oxide biosynthetic process	BP	6.68E-03	1	1
GO:0009703	nitrate reductase (NADH) activity	MF	6.68E-03	1	1
GO:0043546	molybdopterin cofactor binding	MF	6.68E-03	1	1
GO:0050464	nitrate reductase (NADPH) activity	MF	6.68E-03	1	1
GO:0005911	cell-cell junction	CC	6.77E-03	5	177
GO:0030054	cell junction	CC	6.77E-03	5	177
GO:0044459	plasma membrane part	CC	7.14E-03	7	333
GO:0046658	anchored component of plasma membrane	CC	7.22E-03	4	114
GO:0006040	amino sugar metabolic process	BP	8.28E-03	3	62
GO:0016667	oxidoreductase activity, acting on a sulfur group of donors	MF	8.87E-03	4	121
GO:0050896	response to stimulus	BP	9.02E-03	31	3025
GO:0031225	anchored component of membrane	CC	1.02E-02	4	126
GO:0009690	cytokinin metabolic process	BP	1.02E-02	2	23
GO:0010817	regulation of hormone levels	BP	1.08E-02	4	128
GO:0034754	cellular hormone metabolic process	BP	1.20E-02	2	25
GO:0019901	protein kinase binding	MF	1.20E-02	2	25
GO:0007017	microtubule-based process	BP	1.20E-02	5	204
GO:0016854	racemase and epimerase activity	MF	1.30E-02	2	26
GO:0004779	sulfate adenylyltransferase activity	MF	1.33E-02	1	2
GO:0004781	sulfate adenylyltransferase (ATP) activity	MF	1.33E-02	1	2

GO:0047918	GDP-mannose 3,5-epimerase activity	MF	1.33E-02	1	2
GO:0008940	nitrate reductase activity	MF	1.33E-02	1	2
GO:0046857	oxidoreductase activity, acting on other nitrogenous compounds as donors, with NAD or NADP as acceptor	MF	1.33E-02	1	2
GO:0019900	kinase binding	MF	1.39E-02	2	27
GO:0015698	inorganic anion transport	BP	1.44E-02	3	76
GO:0001101	response to acid chemical	BP	1.45E-02	6	295
GO:0019953	sexual reproduction	BP	1.60E-02	2	29
GO:0044703	multi-organism reproductive process	BP	1.81E-02	2	31
GO:0009751	response to salicylic acid	BP	1.88E-02	3	84
GO:0006528	asparagine metabolic process	BP	1.99E-02	1	3
GO:0006529	asparagine biosynthetic process	BP	1.99E-02	1	3
GO:0004066	asparagine synthase (glutamine-hydrolyzing) activity	MF	1.99E-02	1	3
GO:0004604	phosphoadenylyl-sulfate reductase (thioredoxin) activity	MF	1.99E-02	1	3
GO:0047150	betaine-homocysteine S-methyltransferase activity	MF	1.99E-02	1	3
GO:0019419	sulfate reduction	BP	1.99E-02	1	3
GO:0016855	racemase and epimerase activity, acting on amino acids and derivatives	MF	1.99E-02	1	3
GO:0036361	racemase activity, acting on amino acids and derivatives	MF	1.99E-02	1	3
GO:0042073	intraciliary transport	BP	1.99E-02	1	3
GO:0098840	protein transport along microtubule	BP	1.99E-02	1	3
GO:0099118	microtubule-based protein transport	BP	1.99E-02	1	3
GO:0035721	intraciliary retrograde transport	BP	1.99E-02	1	3
GO:0030991	intraciliary transport particle A	CC	1.99E-02	1	3
GO:0043155	negative regulation of photosynthesis, light reaction	BP	1.99E-02	1	3
GO:0010205	photoinhibition	BP	1.99E-02	1	3
GO:0042126	nitrate metabolic process	BP	1.99E-02	1	3
GO:2001057	reactive nitrogen species metabolic process	BP	1.99E-02	1	3
GO:0042128	nitrate assimilation	BP	1.99E-02	1	3
GO:1901136	carbohydrate derivative catabolic process	BP	2.00E-02	3	86
GO:0042445	hormone metabolic process	BP	2.25E-02	3	90
GO:0009725	response to hormone	BP	2.48E-02	7	427
GO:0000427	plastid-encoded plastid RNA polymerase complex	CC	2.65E-02	1	4
GO:0030990	intraciliary transport particle	CC	2.65E-02	1	4
GO:0016661	oxidoreductase activity, acting on other nitrogenous compounds as donors	MF	2.65E-02	1	4
GO:1905156	negative regulation of photosynthesis	BP	2.65E-02	1	4
GO:0015036	disulfide oxidoreductase activity	MF	2.73E-02	3	97

GO:0009753	response to jasmonic acid	BP	2.93E-02	2	40
GO:0007018	microtubule-based movement	BP	2.95E-02	3	100
GO:0015630	microtubule cytoskeleton	CC	3.00E-02	4	175
GO:0005874	microtubule	CC	3.02E-02	3	101
GO:0044036	cell wall macromolecule metabolic process	BP	3.02E-02	3	101
GO:0009719	response to endogenous stimulus	BP	3.04E-02	7	446
GO:0000097	sulfur amino acid biosynthetic process	BP	3.20E-02	2	42
GO:0006952	defense response	BP	3.22E-02	9	656
GO:0008531	riboflavin kinase activity	MF	3.30E-02	1	5
GO:0061512	protein localization to cilium	BP	3.30E-02	1	5
GO:0001666	response to hypoxia	BP	3.30E-02	1	5
GO:0002239	response to oomycetes	BP	3.30E-02	1	5
GO:0002229	defense response to oomycetes	BP	3.30E-02	1	5
GO:0010206	photosystem II repair	BP	3.30E-02	1	5
GO:0005200	structural constituent of cytoskeleton	MF	3.49E-02	2	44
GO:0009416	response to light stimulus	BP	3.51E-02	4	184
GO:0000302	response to reactive oxygen species	BP	3.64E-02	2	45
GO:0006928	movement of cell or subcellular component	BP	3.67E-02	3	109
GO:0009067	aspartate family amino acid biosynthetic process	BP	3.79E-02	2	46
GO:0010304	PSII associated light-harvesting complex II catabolic process	BP	3.94E-02	1	6
GO:0022412	cellular process involved in reproduction in multicellular organism	BP	3.94E-02	1	6
GO:0048235	pollen sperm cell differentiation	BP	3.94E-02	1	6
GO:1903409	reactive oxygen species biosynthetic process	BP	3.94E-02	1	6
GO:0000103	sulfate assimilation	BP	3.94E-02	1	6
GO:0004020	adenylylsulfate kinase activity	MF	3.94E-02	1	6
GO:0031347	regulation of defense response	BP	4.10E-02	3	114
GO:0099081	supramolecular polymer	CC	4.28E-02	3	116
GO:0099512	supramolecular fiber	CC	4.28E-02	3	116
GO:0099513	polymeric cytoskeletal fiber	CC	4.28E-02	3	116
GO:0065008	regulation of biological quality	BP	4.31E-02	9	693
GO:0099080	supramolecular complex	CC	4.38E-02	3	117
GO:0009314	response to radiation	BP	4.40E-02	4	198
GO:0000096	sulfur amino acid metabolic process	BP	4.57E-02	2	51
GO:0042644	chloroplast nucleoid	CC	4.58E-02	1	7
GO:0007276	gamete generation	BP	4.58E-02	1	7
GO:0048232	male gamete generation	BP	4.58E-02	1	7
GO:0012511	monolayer-surrounded lipid storage body	CC	4.58E-02	1	7
GO:0036293	response to decreased oxygen levels	BP	4.58E-02	1	7
GO:0070482	response to oxygen levels	BP	4.58E-02	1	7
GO:0045454	cell redox homeostasis	BP	4.66E-02	3	120
GO:0004791	thioredoxin-disulfide reductase activity	MF	4.73E-02	2	52

GO:0046915	transition metal ion transmembrane transporter activity	MF	4.73E-02	2	52
GO:0009066	aspartate family amino acid metabolic process	BP	4.73E-02	2	52
GO:0009620	response to fungus	BP	4.89E-02	2	53

Supplementary Table S5. 132 GO terms identified from DEGs of heat treatment. The biological functions of DEGs are classified into three main categories such as cellular component (CC), molecular function (MF) and biological process (BP). DE means the number of DEGs in the GO term. N means the number of non-differentially expressed genes in the GO term from genome database. The list is sorted by P-value.

GO id	Annotation	Type	P-value	DE	N
GO:0009266	response to temperature stimulus	BP	1.07E-05	6	104
GO:0009408	response to heat	BP	3.95E-05	4	40
GO:0009628	response to abiotic stimulus	BP	5.05E-05	10	441
GO:0009507	chloroplast	CC	2.26E-04	13	858
GO:0044434	chloroplast part	CC	2.46E-04	9	436
GO:0044435	plastid part	CC	2.76E-04	9	443
GO:0009536	plastid	CC	3.32E-04	13	893
GO:0045543	gibberellin 2-beta-dioxygenase activity	MF	3.36E-04	2	6
GO:0009570	chloroplast stroma	CC	6.50E-04	6	219
GO:0009532	plastid stroma	CC	7.15E-04	6	223
GO:0043436	oxoacid metabolic process	BP	1.41E-03	11	791
GO:0006082	organic acid metabolic process	BP	1.44E-03	11	793
GO:0018210	peptidyl-threonine modification	BP	1.99E-03	2	14
GO:0018107	peptidyl-threonine phosphorylation	BP	1.99E-03	2	14
GO:0009644	response to high light intensity	BP	2.29E-03	2	15
GO:0045543	gibberellin metabolic process	BP	2.94E-03	2	17
GO:0019752	carboxylic acid metabolic process	BP	3.16E-03	10	750
GO:0004366	glycerol-3-phosphate O-acyltransferase activity	MF	4.78E-03	1	1
GO:1903600	glutaminase complex	CC	4.78E-03	1	1
GO:0052635	C-20 gibberellin 2-beta-dioxygenase activity	MF	4.78E-03	1	1
GO:0046209	nitric oxide metabolic process	BP	4.78E-03	1	1
GO:0006809	nitric oxide biosynthetic process	BP	4.78E-03	1	1
GO:0009703	nitrate reductase (NADH) activity	MF	4.78E-03	1	1
GO:0043546	molybdopterin cofactor binding	MF	4.78E-03	1	1
GO:0050464	nitrate reductase (NADPH) activity	MF	4.78E-03	1	1
GO:0016101	diterpenoid metabolic process	BP	4.92E-03	2	22
GO:0016706	oxidoreductase activity, acting on paired donors, with incorporation or reduction of molecular oxygen, 2-oxoglutarate as one donor, and incorporation of one atom each of oxygen into both donors	MF	5.37E-03	2	23
GO:0044281	small molecule metabolic process	BP	7.17E-03	13	1263
GO:0008237	metallopeptidase activity	MF	7.41E-03	3	83
GO:0050896	response to stimulus	BP	7.67E-03	24	3025

GO:0006457	protein folding	BP	8.69E-03	4	168
GO:0006520	cellular amino acid metabolic process	BP	9.09E-03	6	373
GO:0004359	glutaminase activity	MF	9.55E-03	1	2
GO:0006428	isoleucyl-tRNA aminoacylation	BP	9.55E-03	1	2
GO:0004822	isoleucine-tRNA ligase activity	MF	9.55E-03	1	2
GO:0004779	sulfate adenylyltransferase activity	MF	9.55E-03	1	2
GO:0004781	sulfate adenylyltransferase (ATP) activity	MF	9.55E-03	1	2
GO:0017102	methionyl glutamyl tRNA synthetase complex	CC	9.55E-03	1	2
GO:0004107	chorismate synthase activity	MF	9.55E-03	1	2
GO:0008940	nitrate reductase activity	MF	9.55E-03	1	2
GO:0046857	oxidoreductase activity, acting on other nitrogenous compounds as donors, with NAD or NADP as acceptor	MF	9.55E-03	1	2
GO:0009642	response to light intensity	BP	1.02E-02	2	32
GO:0006418	tRNA aminoacylation for protein translation	BP	1.04E-02	3	94
GO:0000049	tRNA binding	MF	1.09E-02	2	33
GO:0043038	amino acid activation	BP	1.10E-02	3	96
GO:0043039	tRNA aminoacylation	BP	1.10E-02	3	96
GO:1901700	response to oxygen-containing compound	BP	1.14E-02	6	392
GO:0009416	response to light stimulus	BP	1.18E-02	4	184
GO:0009941	chloroplast envelope	CC	1.34E-02	4	191
GO:0051082	unfolded protein binding	MF	1.40E-02	3	105
GO:0070084	protein initiator methionine removal	BP	1.43E-02	1	3
GO:0006430	lysyl-tRNA aminoacylation	BP	1.43E-02	1	3
GO:0004824	lysine-tRNA ligase activity	MF	1.43E-02	1	3
GO:0008614	pyridoxine metabolic process	BP	1.43E-02	1	3
GO:0016688	L-ascorbate peroxidase activity	MF	1.43E-02	1	3
GO:0016855	racemase and epimerase activity, acting on amino acids and derivatives	MF	1.43E-02	1	3
GO:0036361	racemase activity, acting on amino acids and derivatives	MF	1.43E-02	1	3
GO:0043155	negative regulation of photosynthesis, light reaction	BP	1.43E-02	1	3
GO:0010205	photoinhibition	BP	1.43E-02	1	3
GO:0004048	anthranilate phosphoribosyltransferase activity	MF	1.43E-02	1	3
GO:0042126	nitrate metabolic process	BP	1.43E-02	1	3
GO:2001057	reactive nitrogen species metabolic process	BP	1.43E-02	1	3
GO:0042128	nitrate assimilation	BP	1.43E-02	1	3
GO:0009526	plastid envelope	CC	1.49E-02	4	197
GO:0009073	aromatic amino acid family biosynthetic process	BP	1.50E-02	2	39
GO:0009314	response to radiation	BP	1.51E-02	4	198
GO:0098661	inorganic anion transmembrane transport	BP	1.65E-02	2	41
GO:0051186	cofactor metabolic process	BP	1.78E-02	5	315
GO:0046341	CDP-diacylglycerol metabolic process	BP	1.90E-02	1	4
GO:0016024	CDP-diacylglycerol biosynthetic process	BP	1.90E-02	1	4

GO:0004751	ribose-5-phosphate isomerase activity	MF	1.90E-02	1	4
GO:0017101	aminoacyl-tRNA synthetase multienzyme complex	CC	1.90E-02	1	4
GO:0016661	oxidoreductase activity, acting on other nitrogenous compounds as donors	MF	1.90E-02	1	4
GO:1905156	negative regulation of photosynthesis	BP	1.90E-02	1	4
GO:0000302	response to reactive oxygen species	BP	1.96E-02	2	45
GO:0006081	cellular aldehyde metabolic process	BP	2.22E-02	2	48
GO:0030151	molybdenum ion binding	MF	2.37E-02	1	5
GO:0000380	alternative mRNA splicing, via spliceosome	BP	2.37E-02	1	5
GO:0015114	phosphate ion transmembrane transporter activity	MF	2.37E-02	1	5
GO:0005504	fatty acid binding	MF	2.37E-02	1	5
GO:0016103	diterpenoid catabolic process	BP	2.37E-02	1	5
GO:0016115	terpenoid catabolic process	BP	2.37E-02	1	5
GO:0045487	gibberellin catabolic process	BP	2.37E-02	1	5
GO:0052634	C-19 gibberellin 2-beta-dioxygenase activity	MF	2.37E-02	1	5
GO:0034605	cellular response to heat	BP	2.37E-02	1	5
GO:0010206	photosystem II repair	BP	2.37E-02	1	5
GO:0010304	PSII associated light-harvesting complex II catabolic process	BP	2.84E-02	1	6
GO:0009052	pentose-phosphate shunt, non-oxidative branch	BP	2.84E-02	1	6
GO:0097428	protein maturation by iron-sulfur cluster transfer	BP	2.84E-02	1	6
GO:1903409	reactive oxygen species biosynthetic process	BP	2.84E-02	1	6
GO:0000103	sulfate assimilation	BP	2.84E-02	1	6
GO:0004020	adenylylsulfate kinase activity	MF	2.84E-02	1	6
GO:0045430	chalcone isomerase activity	MF	2.84E-02	1	6
GO:0050897	cobalt ion binding	MF	2.84E-02	1	6
GO:0008300	isoprenoid catabolic process	BP	2.84E-02	1	6
GO:0009269	response to desiccation	BP	2.84E-02	1	6
GO:1901698	response to nitrogen compound	BP	2.95E-02	2	56
GO:0004222	metalloendopeptidase activity	MF	3.05E-02	2	57
GO:0046471	phosphatidylglycerol metabolic process	BP	3.30E-02	1	7
GO:0006655	phosphatidylglycerol biosynthetic process	BP	3.30E-02	1	7
GO:0010319	stromule	CC	3.30E-02	1	7
GO:0016872	intramolecular lyase activity	MF	3.30E-02	1	7
GO:0033293	monocarboxylic acid binding	MF	3.30E-02	1	7
GO:0015103	inorganic anion transmembrane transporter activity	MF	3.56E-02	2	62
GO:0009534	chloroplast thylakoid	CC	3.66E-02	3	152
GO:0031976	plastid thylakoid	CC	3.72E-02	3	153
GO:0042548	regulation of photosynthesis, light reaction	BP	3.76E-02	1	8
GO:0043467	regulation of generation of precursor metabolites and energy	BP	3.76E-02	1	8
GO:0030091	protein repair	BP	3.76E-02	1	8
GO:1901677	phosphate transmembrane transporter activity	MF	3.76E-02	1	8

GO:0008534	oxidized purine nucleobase lesion DNA N-glycosylase activity	MF	3.76E-02	1	8
GO:0047746	chlorophyllase activity	MF	3.76E-02	1	8
GO:0004721	phosphoprotein phosphatase activity	MF	3.84E-02	3	155
GO:0006721	terpenoid metabolic process	BP	3.88E-02	2	65
GO:0009072	aromatic amino acid family metabolic process	BP	4.21E-02	2	68
GO:0004867	serine-type endopeptidase inhibitor activity	MF	4.23E-02	1	9
GO:0070940	dephosphorylation of RNA polymerase II C-terminal domain	BP	4.23E-02	1	9
GO:0008420	CTD phosphatase activity	MF	4.23E-02	1	9
GO:0071941	nitrogen cycle metabolic process	BP	4.23E-02	1	9
GO:0010167	response to nitrate	BP	4.23E-02	1	9
GO:0004130	cytochrome-c peroxidase activity	MF	4.23E-02	1	9
GO:0000702	oxidized base lesion DNA N-glycosylase activity	MF	4.23E-02	1	9
GO:0006470	protein dephosphorylation	BP	4.29E-02	3	162
GO:0018105	peptidyl-serine phosphorylation	BP	4.32E-02	2	69
GO:0010035	response to inorganic substance	BP	4.62E-02	3	167
GO:0035435	phosphate ion transmembrane transport	BP	4.68E-02	1	10
GO:0042542	response to hydrogen peroxide	BP	4.68E-02	1	10
GO:0042816	vitamin B6 metabolic process	BP	4.68E-02	1	10
GO:0042819	vitamin B6 biosynthetic process	BP	4.68E-02	1	10
GO:0042822	pyridoxal phosphate metabolic process	BP	4.68E-02	1	10
GO:0042823	pyridoxal phosphate biosynthetic process	BP	4.68E-02	1	10
GO:0018209	peptidyl-serine modification	BP	4.90E-02	2	74

Supplementary Table S6. 534 GO terms identified from DEGs of drought/heat treatment.

The biological functions of DEGs are classified into three main categories such as cellular component (CC), molecular function (MF) and biological process (BP). DE means the number of DEGs in the GO term. N means the number of non-differentially expressed genes in the GO term from genome database. The list is sorted by P-value.

GO id	Annotation	Type	P-value	DE	N
GO:0044281	small molecule metabolic process	BP	4.70E-12	179	1263
GO:0019752	carboxylic acid metabolic process	BP	1.60E-09	113	750
GO:0009628	response to abiotic stimulus	BP	5.85E-09	75	441
GO:0043436	oxoacid metabolic process	BP	9.16E-09	115	791
GO:0006082	organic acid metabolic process	BP	1.06E-08	115	793
GO:0005975	carbohydrate metabolic process	BP	3.43E-08	135	994
GO:0009813	flavonoid biosynthetic process	BP	4.48E-07	12	26
GO:0044710	single-organism metabolic process	BP	5.06E-07	413	3907
GO:0009812	flavonoid metabolic process	BP	9.04E-07	13	32
GO:0000502	proteasome complex	CC	9.30E-07	19	64
GO:1905369	endopeptidase complex	CC	9.30E-07	19	64
GO:0016052	carbohydrate catabolic process	BP	1.35E-06	41	219
GO:0044723	single-organism carbohydrate metabolic process	BP	1.44E-06	64	408
GO:0022891	substrate-specific transmembrane transporter activity	MF	2.43E-06	112	851
GO:0009408	response to heat	BP	2.87E-06	14	40
GO:0019693	ribose phosphate metabolic process	BP	4.37E-06	42	237
GO:0044711	single-organism biosynthetic process	BP	4.85E-06	164	1372
GO:1905368	peptidase complex	CC	6.01E-06	20	78
GO:0044283	small molecule biosynthetic process	BP	6.92E-06	66	445
GO:0006811	ion transport	BP	9.68E-06	117	925
GO:0006006	glucose metabolic process	BP	1.03E-05	14	44
GO:0072521	purine-containing compound metabolic process	BP	1.04E-05	40	229
GO:0009150	purine ribonucleotide metabolic process	BP	1.15E-05	36	198
GO:0006091	generation of precursor metabolites and energy	BP	1.33E-05	44	264
GO:0009199	ribonucleoside triphosphate metabolic process	BP	1.48E-05	32	169
GO:0009205	purine ribonucleoside triphosphate metabolic process	BP	1.60E-05	31	162
GO:0006163	purine nucleotide metabolic process	BP	2.02E-05	36	203
GO:0008150	biological_process	BP	2.04E-05	1450	16168
GO:0022857	transmembrane transporter activity	MF	2.16E-05	144	1208
GO:0051213	dioxygenase activity	MF	2.25E-05	19	78

GO:0009144	purine nucleoside triphosphate metabolic process	BP	2.34E-05	31	165
GO:0006732	coenzyme metabolic process	BP	2.44E-05	39	229
GO:0009126	purine nucleoside monophosphate metabolic process	BP	3.05E-05	32	175
GO:0009167	purine ribonucleoside monophosphate metabolic process	BP	3.05E-05	32	175
GO:0016053	organic acid biosynthetic process	BP	3.29E-05	53	351
GO:0046394	carboxylic acid biosynthetic process	BP	3.29E-05	53	351
GO:0006753	nucleoside phosphate metabolic process	BP	3.38E-05	48	308
GO:0006541	glutamine metabolic process	BP	3.53E-05	7	13
GO:0009117	nucleotide metabolic process	BP	3.54E-05	47	300
GO:0009259	ribonucleotide metabolic process	BP	3.79E-05	37	217
GO:0015980	energy derivation by oxidation of organic compounds	BP	3.81E-05	24	116
GO:0005215	transporter activity	MF	3.83E-05	169	1475
GO:0005996	monosaccharide metabolic process	BP	3.96E-05	19	81
GO:0070003	threonine-type peptidase activity	MF	4.20E-05	9	22
GO:0004298	threonine-type endopeptidase activity	MF	4.20E-05	9	22
GO:0055085	transmembrane transport	BP	4.46E-05	147	1256
GO:0022892	substrate-specific transporter activity	MF	5.07E-05	117	960
GO:0015698	inorganic anion transport	BP	5.47E-05	18	76
GO:0009141	nucleoside triphosphate metabolic process	BP	6.04E-05	32	181
GO:0019318	hexose metabolic process	BP	6.23E-05	17	70
GO:0005839	proteasome core complex	CC	6.38E-05	9	23
GO:0016706	oxidoreductase activity, acting on paired donors, with incorporation or reduction of molecular oxygen, 2-oxoglutarate as one donor, and incorporation of one atom each of oxygen into both donors	MF	6.38E-05	9	23
GO:0072522	purine-containing compound biosynthetic process	BP	6.76E-05	20	91
GO:0005976	polysaccharide metabolic process	BP	7.04E-05	53	361
GO:0046034	ATP metabolic process	BP	7.23E-05	28	151
GO:0009152	purine ribonucleotide biosynthetic process	BP	7.88E-05	18	78
GO:0009145	purine nucleoside triphosphate biosynthetic process	BP	8.24E-05	14	52
GO:0009206	purine ribonucleoside triphosphate biosynthetic process	BP	8.24E-05	14	52
GO:0006820	anion transport	BP	8.56E-05	46	302
GO:0031226	intrinsic component of plasma membrane	CC	9.05E-05	45	294
GO:0009201	ribonucleoside triphosphate biosynthetic process	BP	9.50E-05	15	59
GO:0000272	polysaccharide catabolic process	BP	9.81E-05	26	138
GO:0042221	response to chemical	BP	1.02E-04	120	1006

GO:0006164	purine nucleotide biosynthetic process	BP	1.12E-04	18	80
GO:0055086	nucleobase-containing small molecule metabolic process	BP	1.16E-04	52	359
GO:0009142	nucleoside triphosphate biosynthetic process	BP	1.17E-04	15	60
GO:0044763	single-organism cellular process	BP	1.26E-04	376	3723
GO:0034220	ion transmembrane transport	BP	1.27E-04	80	620
GO:0071365	cellular response to auxin stimulus	BP	1.31E-04	17	74
GO:0009734	auxin-activated signaling pathway	BP	1.31E-04	17	74
GO:1901575	organic substance catabolic process	BP	1.44E-04	141	1226
GO:0009123	nucleoside monophosphate metabolic process	BP	1.52E-04	33	198
GO:0031967	organelle envelope	CC	1.63E-04	68	511
GO:0031975	envelope	CC	1.63E-04	68	511
GO:0019637	organophosphate metabolic process	BP	1.67E-04	67	502
GO:0009161	ribonucleoside monophosphate metabolic process	BP	1.90E-04	32	192
GO:0016616	oxidoreductase activity, acting on the CH-OH group of donors, NAD or NADP as acceptor	MF	1.93E-04	24	128
GO:0019773	proteasome core complex, alpha-subunit complex	CC	2.03E-04	5	8
GO:0080167	response to karrikin	BP	2.26E-04	6	12
GO:0051186	cofactor metabolic process	BP	2.32E-04	46	315
GO:0015075	ion transmembrane transporter activity	MF	2.51E-04	87	701
GO:0009060	aerobic respiration	BP	2.66E-04	13	51
GO:0006101	citrate metabolic process	BP	3.02E-04	11	39
GO:0006520	cellular amino acid metabolic process	BP	3.04E-04	52	373
GO:0032787	monocarboxylic acid metabolic process	BP	3.33E-04	46	320
GO:0009056	catabolic process	BP	3.54E-04	164	1489
GO:0005982	starch metabolic process	BP	3.64E-04	9	28
GO:0010035	response to inorganic substance	BP	4.19E-04	28	167
GO:0008272	sulfate transport	BP	4.23E-04	8	23
GO:0009127	purine nucleoside monophosphate biosynthetic process	BP	4.30E-04	15	67
GO:0009168	purine ribonucleoside monophosphate biosynthetic process	BP	4.30E-04	15	67
GO:0044459	plasma membrane part	CC	4.38E-04	47	333
GO:0005740	mitochondrial envelope	CC	4.52E-04	35	227
GO:0009266	response to temperature stimulus	BP	4.53E-04	20	104
GO:0009057	macromolecule catabolic process	BP	4.62E-04	102	863
GO:0009260	ribonucleotide biosynthetic process	BP	4.90E-04	19	97
GO:0046390	ribose phosphate biosynthetic process	BP	4.90E-04	19	97
GO:1902578	single-organism localization	BP	5.22E-04	115	997
GO:0044765	single-organism transport	BP	5.29E-04	112	967
GO:0008509	anion transmembrane transporter activity	MF	5.79E-04	35	230
GO:0008652	cellular amino acid biosynthetic process	BP	6.19E-04	28	171
GO:0004774	succinate-CoA ligase activity	MF	6.21E-04	3	3

GO:0004775	succinate-CoA ligase (ADP-forming) activity	MF	6.21E-04	3	3
GO:0051234	establishment of localization	BP	6.26E-04	247	2390
GO:0009629	response to gravity	BP	6.32E-04	6	14
GO:0006084	acetyl-CoA metabolic process	BP	6.32E-04	6	14
GO:0005887	integral component of plasma membrane	CC	6.55E-04	29	180
GO:0042451	purine nucleoside biosynthetic process	BP	6.56E-04	7	19
GO:0046129	purine ribonucleoside biosynthetic process	BP	6.56E-04	7	19
GO:0006073	cellular glucan metabolic process	BP	6.81E-04	32	206
GO:1902600	hydrogen ion transmembrane transport	BP	6.86E-04	22	123
GO:0005743	mitochondrial inner membrane	CC	6.87E-04	30	189
GO:0006542	glutamine biosynthetic process	BP	6.90E-04	4	6
GO:0016211	ammonia ligase activity	MF	6.90E-04	4	6
GO:0016880	acid-ammonia (or amide) ligase activity	MF	6.90E-04	4	6
GO:0004356	glutamate-ammonia ligase activity	MF	6.90E-04	4	6
GO:0006810	transport	BP	6.94E-04	244	2362
GO:0031966	mitochondrial membrane	CC	7.02E-04	33	215
GO:0072350	tricarboxylic acid metabolic process	BP	7.54E-04	11	43
GO:0010033	response to organic substance	BP	7.74E-04	75	608
GO:0044262	cellular carbohydrate metabolic process	BP	7.89E-04	47	342
GO:0044434	chloroplast part	CC	8.19E-04	57	436
GO:0044042	glucan metabolic process	BP	8.96E-04	33	218
GO:0010928	regulation of auxin mediated signaling pathway	BP	9.35E-04	7	20
GO:0031595	nuclear proteasome complex	CC	9.77E-04	6	15
GO:0005838	proteasome regulatory particle	CC	1.02E-03	10	38
GO:0022624	proteasome accessory complex	CC	1.02E-03	10	38
GO:0006099	tricarboxylic acid cycle	BP	1.02E-03	10	38
GO:0019866	organelle inner membrane	CC	1.12E-03	32	212
GO:0044724	single-organism carbohydrate catabolic process	BP	1.12E-03	17	88
GO:0006754	ATP biosynthetic process	BP	1.14E-03	11	45
GO:0044429	mitochondrial part	CC	1.15E-03	42	302
GO:0051179	localization	BP	1.16E-03	250	2449
GO:0016836	hydro-lyase activity	MF	1.19E-03	13	59
GO:0044435	plastid part	CC	1.20E-03	57	443
GO:0009073	aromatic amino acid family biosynthetic process	BP	1.27E-03	10	39
GO:0017025	TBP-class protein binding	MF	1.30E-03	7	21
GO:0051082	unfolded protein binding	MF	1.34E-03	19	105
GO:0006085	acetyl-CoA biosynthetic process	BP	1.34E-03	5	11
GO:0044699	single-organism process	BP	1.41E-03	699	7499
GO:0019252	starch biosynthetic process	BP	1.45E-03	6	16
GO:0016872	intramolecular lyase activity	MF	1.50E-03	4	7
GO:1901700	response to oxygen-containing compound	BP	1.66E-03	51	392
GO:0005515	protein binding	MF	1.70E-03	152	1416
GO:1902358	sulfate transmembrane transport	BP	1.77E-03	7	22

GO:0015116	sulfate transmembrane transporter activity	MF	1.77E-03	7	22
GO:0042578	phosphoric ester hydrolase activity	MF	1.84E-03	44	328
GO:0044272	sulfur compound biosynthetic process	BP	1.88E-03	18	100
GO:0009755	hormone-mediated signaling pathway	BP	1.90E-03	31	210
GO:0098661	inorganic anion transmembrane transport	BP	1.92E-03	10	41
GO:0015103	inorganic anion transmembrane transporter activity	MF	1.92E-03	13	62
GO:0006793	phosphorus metabolic process	BP	2.05E-03	250	2475
GO:0008810	cellulase activity	MF	2.08E-03	6	17
GO:0008271	secondary active sulfate transmembrane transporter activity	MF	2.08E-03	6	17
GO:0045333	cellular respiration	BP	2.09E-03	17	93
GO:0016614	oxidoreductase activity, acting on CH-OH group of donors	MF	2.11E-03	28	185
GO:0098660	inorganic ion transmembrane transport	BP	2.12E-03	48	368
GO:0015562	efflux transmembrane transporter activity	MF	2.14E-03	5	12
GO:0080161	auxin transmembrane transporter activity	MF	2.14E-03	5	12
GO:0010329	auxin efflux transmembrane transporter activity	MF	2.14E-03	5	12
GO:0035384	thioester biosynthetic process	BP	2.14E-03	5	12
GO:0071616	acyl-CoA biosynthetic process	BP	2.14E-03	5	12
GO:0016624	oxidoreductase activity, acting on the aldehyde or oxo group of donors, disulfide as acceptor	MF	2.14E-03	5	12
GO:0006457	protein folding	BP	2.18E-03	26	168
GO:0006818	hydrogen transport	BP	2.20E-03	31	212
GO:0015992	proton transport	BP	2.20E-03	31	212
GO:0016853	isomerase activity	MF	2.27E-03	39	285
GO:0009719	response to endogenous stimulus	BP	2.29E-03	56	446
GO:0009725	response to hormone	BP	2.32E-03	54	427
GO:0004491	methylmalonate-semialdehyde dehydrogenase (acylating) activity	MF	2.33E-03	3	4
GO:0047769	arogenate dehydratase activity	MF	2.33E-03	3	4
GO:0016405	CoA-ligase activity	MF	2.33E-03	3	4
GO:0009735	response to cytokinin	BP	2.33E-03	10	42
GO:0072524	pyridine-containing compound metabolic process	BP	2.34E-03	19	110
GO:0003674	molecular_function	MF	2.34E-03	1493	169556
GO:0005977	glycogen metabolic process	BP	2.35E-03	7	23
GO:0006112	energy reserve metabolic process	BP	2.35E-03	7	23
GO:0065004	protein-DNA complex assembly	BP	2.35E-03	17	94
GO:0003824	catalytic activity	MF	2.42E-03	971	10699
GO:0046128	purine ribonucleoside metabolic process	BP	2.66E-03	9	36
GO:0006812	cation transport	BP	2.69E-03	68	567

GO:0016051	carbohydrate biosynthetic process	BP	2.71E-03	35	251
GO:0098656	anion transmembrane transport	BP	2.73E-03	30	206
GO:0032870	cellular response to hormone stimulus	BP	2.75E-03	31	215
GO:0005750	mitochondrial respiratory chain complex III	CC	2.80E-03	4	8
GO:0006086	acetyl-CoA biosynthetic process from pyruvate	BP	2.80E-03	4	8
GO:0004738	pyruvate dehydrogenase activity	MF	2.80E-03	4	8
GO:0004739	pyruvate dehydrogenase (acetyl-transferring) activity	MF	2.80E-03	4	8
GO:0006733	oxidoreduction coenzyme metabolic process	BP	2.89E-03	19	112
GO:0006817	phosphate ion transport	BP	2.90E-03	6	18
GO:0070069	cytochrome complex	CC	2.90E-03	6	18
GO:0071495	cellular response to endogenous stimulus	BP	3.17E-03	31	217
GO:1901135	carbohydrate derivative metabolic process	BP	3.21E-03	73	621
GO:0043424	protein histidine kinase binding	MF	3.24E-03	5	13
GO:0010315	auxin efflux	BP	3.24E-03	5	13
GO:0046500	S-adenosylmethionine metabolic process	BP	3.24E-03	5	13
GO:0072348	sulfur compound transport	BP	3.68E-03	8	31
GO:0009124	nucleoside monophosphate biosynthetic process	BP	3.72E-03	16	90
GO:0009312	oligosaccharide biosynthetic process	BP	3.89E-03	11	52
GO:1901605	alpha-amino acid metabolic process	BP	3.92E-03	30	211
GO:0098805	whole membrane	CC	3.93E-03	47	370
GO:0071368	cellular response to cytokinin stimulus	BP	3.93E-03	6	19
GO:0009736	cytokinin-activated signaling pathway	BP	3.93E-03	6	19
GO:0006165	nucleoside diphosphate phosphorylation	BP	3.95E-03	13	67
GO:0009251	glucan catabolic process	BP	3.95E-03	9	38
GO:0033178	proton-transporting two-sector ATPase complex, catalytic domain	CC	3.97E-03	7	25
GO:1901293	nucleoside phosphate biosynthetic process	BP	3.97E-03	21	132
GO:0019362	pyridine nucleotide metabolic process	BP	4.12E-03	17	99
GO:0046496	nicotinamide nucleotide metabolic process	BP	4.12E-03	17	99
GO:0015078	hydrogen ion transmembrane transporter activity	MF	4.15E-03	20	124
GO:0016791	phosphatase activity	MF	4.25E-03	38	286
GO:0009072	aromatic amino acid family metabolic process	BP	4.50E-03	13	68
GO:0019829	cation-transporting ATPase activity	MF	4.58E-03	17	100
GO:0042625	ATPase coupled ion transmembrane transporter activity	MF	4.58E-03	17	100
GO:0045490	pectin catabolic process	BP	4.64E-03	14	76
GO:0009156	ribonucleoside monophosphate biosynthetic process	BP	4.68E-03	15	84
GO:0051275	beta-glucan catabolic process	BP	4.68E-03	5	14
GO:0030245	cellulose catabolic process	BP	4.68E-03	5	14
GO:0045275	respiratory chain complex III	CC	4.70E-03	4	9
GO:0009071	serine family amino acid catabolic process	BP	4.70E-03	4	9

GO:0042278	purine nucleoside metabolic process	BP	4.76E-03	9	39
GO:0009733	response to auxin	BP	4.80E-03	25	169
GO:0009507	chloroplast	CC	5.13E-03	95	858
GO:0006839	mitochondrial transport	BP	5.22E-03	19	118
GO:0009526	plastid envelope	CC	5.22E-03	28	197
GO:0055114	oxidation-reduction process	BP	5.29E-03	206	2041
GO:0016311	dephosphorylation	BP	5.37E-03	40	309
GO:1902223	erythrose 4-phosphate/phosphoenolpyruvate family amino acid biosynthetic process	BP	5.44E-03	3	5
GO:0009094	L-phenylalanine biosynthetic process	BP	5.44E-03	3	5
GO:0016878	acid-thiol ligase activity	MF	5.44E-03	3	5
GO:0070897	DNA-templated transcriptional preinitiation complex assembly	BP	5.56E-03	8	33
GO:0071824	protein-DNA complex subunit organization	BP	5.62E-03	17	102
GO:0031090	organelle membrane	CC	5.65E-03	81	717
GO:0009132	nucleoside diphosphate metabolic process	BP	5.82E-03	13	70
GO:0006629	lipid metabolic process	BP	6.20E-03	86	771
GO:0022853	active ion transmembrane transporter activity	MF	6.21E-03	17	103
GO:0006796	phosphate-containing compound metabolic process	BP	6.28E-03	241	2432
GO:0030163	protein catabolic process	BP	6.34E-03	67	578
GO:0009644	response to high light intensity	BP	6.54E-03	5	15
GO:0006090	pyruvate metabolic process	BP	7.09E-03	16	96
GO:0009165	nucleotide biosynthetic process	BP	7.09E-03	20	130
GO:0046939	nucleotide phosphorylation	BP	7.28E-03	15	88
GO:0009590	detection of gravity	BP	7.28E-03	2	2
GO:0004614	phosphoglucomutase activity	MF	7.28E-03	2	2
GO:0006424	glutamyl-tRNA aminoacylation	BP	7.28E-03	2	2
GO:0004818	glutamate-tRNA ligase activity	MF	7.28E-03	2	2
GO:0045486	naringenin 3-dioxygenase activity	MF	7.28E-03	2	2
GO:0004779	sulfate adenylyltransferase activity	MF	7.28E-03	2	2
GO:0004781	sulfate adenylyltransferase (ATP) activity	MF	7.28E-03	2	2
GO:0016210	naringenin-chalcone synthase activity	MF	7.28E-03	2	2
GO:0008897	holo-[acyl-carrier-protein] synthase activity	MF	7.28E-03	2	2
GO:0004776	succinate-CoA ligase (GDP-forming) activity	MF	7.28E-03	2	2
GO:1901070	guanosine-containing compound biosynthetic process	BP	7.30E-03	4	10
GO:0035435	phosphate ion transmembrane transport	BP	7.30E-03	4	10
GO:0042542	response to hydrogen peroxide	BP	7.30E-03	4	10
GO:0031492	nucleosomal DNA binding	MF	7.30E-03	4	10
GO:1902495	transmembrane transporter complex	CC	7.30E-03	4	10
GO:0009416	response to light stimulus	BP	7.47E-03	26	184
GO:0072330	monocarboxylic acid biosynthetic process	BP	7.98E-03	22	149
GO:0055044	symplast	CC	8.05E-03	25	176
GO:0009506	plasmodesma	CC	8.05E-03	25	176

GO:0044264	cellular polysaccharide metabolic process	BP	8.27E-03	32	241
GO:0006721	terpenoid metabolic process	BP	8.27E-03	12	65
GO:0009311	oligosaccharide metabolic process	BP	8.33E-03	13	73
GO:0005911	cell-cell junction	CC	8.64E-03	25	177
GO:0030054	cell junction	CC	8.64E-03	25	177
GO:0043650	dicarboxylic acid biosynthetic process	BP	8.67E-03	6	22
GO:0060260	regulation of transcription initiation from RNA polymerase II promoter	BP	8.85E-03	5	16
GO:2000142	regulation of DNA-templated transcription, initiation	BP	8.85E-03	5	16
GO:2000144	positive regulation of DNA-templated transcription, initiation	BP	8.85E-03	5	16
GO:0060261	positive regulation of transcription initiation from RNA polymerase II promoter	BP	8.85E-03	5	16
GO:0015866	ADP transport	BP	8.85E-03	5	16
GO:0015662	ATPase activity, coupled to transmembrane movement of ions, phosphorylative mechanism	MF	9.30E-03	9	43
GO:0046351	disaccharide biosynthetic process	BP	9.64E-03	8	36
GO:0015985	energy coupled proton transport, down electrochemical gradient	BP	9.64E-03	8	36
GO:0015986	ATP synthesis coupled proton transport	BP	9.64E-03	8	36
GO:0032993	protein-DNA complex	CC	9.89E-03	15	91
GO:0010393	galacturonan metabolic process	BP	9.89E-03	15	91
GO:0045488	pectin metabolic process	BP	9.89E-03	15	91
GO:0044255	cellular lipid metabolic process	BP	9.97E-03	58	499
GO:0030100	regulation of endocytosis	BP	1.02E-02	3	6
GO:0045430	chalcone isomerase activity	MF	1.02E-02	3	6
GO:0006633	fatty acid biosynthetic process	BP	1.03E-02	18	117
GO:0016879	ligase activity, forming carbon-nitrogen bonds	MF	1.04E-02	11	59
GO:0009415	response to water	BP	1.05E-02	12	67
GO:0071470	cellular response to osmotic stress	BP	1.07E-02	4	11
GO:0009927	histidine phosphotransfer kinase activity	MF	1.07E-02	4	11
GO:0006334	nucleosome assembly	BP	1.08E-02	9	44
GO:0009536	plastid	CC	1.09E-02	96	893
GO:0044275	cellular carbohydrate catabolic process	BP	1.15E-02	10	52
GO:1901682	sulfur compound transmembrane transporter activity	MF	1.16E-02	7	30
GO:0031407	oxylipin metabolic process	BP	1.17E-02	5	17
GO:0031408	oxylipin biosynthetic process	BP	1.17E-02	5	17
GO:0046417	chorismate metabolic process	BP	1.17E-02	5	17
GO:0001101	response to acid chemical	BP	1.17E-02	37	295
GO:0070887	cellular response to chemical stimulus	BP	1.18E-02	49	413
GO:0000786	nucleosome	CC	1.18E-02	11	60
GO:0009941	chloroplast envelope	CC	1.19E-02	26	191
GO:0004722	protein serine/threonine phosphatase activity	MF	1.20E-02	15	93

GO:0090662	ATP hydrolysis coupled transmembrane transport	BP	1.20E-02	15	93
GO:0099131	ATP hydrolysis coupled ion transmembrane transport	BP	1.20E-02	15	93
GO:0099132	ATP hydrolysis coupled cation transmembrane transport	BP	1.20E-02	15	93
GO:1901607	alpha-amino acid biosynthetic process	BP	1.25E-02	21	146
GO:0005618	cell wall	CC	1.28E-02	40	326
GO:0030312	external encapsulating structure	CC	1.28E-02	40	326
GO:0005984	disaccharide metabolic process	BP	1.31E-02	10	53
GO:0009069	serine family amino acid metabolic process	BP	1.31E-02	10	53
GO:0008324	cation transmembrane transporter activity	MF	1.34E-02	51	436
GO:0046933	proton-transporting ATP synthase activity, rotational mechanism	MF	1.35E-02	6	24
GO:0006790	sulfur compound metabolic process	BP	1.43E-02	37	299
GO:0098655	cation transmembrane transport	BP	1.44E-02	44	368
GO:0044257	cellular protein catabolic process	BP	1.47E-02	57	499
GO:0006757	ATP generation from ADP	BP	1.50E-02	11	62
GO:0046031	ADP metabolic process	BP	1.50E-02	11	62
GO:0006096	glycolytic process	BP	1.50E-02	11	62
GO:0006122	mitochondrial electron transport, ubiquinol to cytochrome c	BP	1.50E-02	4	12
GO:0005978	glycogen biosynthetic process	BP	1.50E-02	4	12
GO:0009630	gravitropism	BP	1.50E-02	4	12
GO:0045898	regulation of RNA polymerase II transcriptional preinitiation complex assembly	BP	1.50E-02	4	12
GO:0045899	positive regulation of RNA polymerase II transcriptional preinitiation complex assembly	BP	1.50E-02	4	12
GO:0006970	response to osmotic stress	BP	1.53E-02	17	113
GO:0042775	mitochondrial ATP synthesis coupled electron transport	BP	1.65E-02	6	25
GO:0019901	protein kinase binding	MF	1.65E-02	6	25
GO:0006637	acyl-CoA metabolic process	BP	1.65E-02	6	25
GO:0035383	thioester metabolic process	BP	1.65E-02	6	25
GO:0033356	UDP-L-arabinose metabolic process	BP	1.67E-02	3	7
GO:0052691	UDP-arabinopyranose mutase activity	MF	1.67E-02	3	7
GO:0006546	glycine catabolic process	BP	1.67E-02	3	7
GO:0010319	stromule	CC	1.67E-02	3	7
GO:0019187	beta-1,4-mannosyltransferase activity	MF	1.67E-02	3	7
GO:0051753	mannan synthase activity	MF	1.67E-02	3	7
GO:0006183	GTP biosynthetic process	BP	1.67E-02	3	7
GO:0006388	tRNA splicing, via endonucleolytic cleavage and ligation	BP	1.67E-02	3	7
GO:0000788	nuclear nucleosome	CC	1.67E-02	3	7
GO:0042545	cell wall modification	BP	1.68E-02	11	63

GO:0051603	proteolysis involved in cellular protein catabolic process	BP	1.71E-02	56	493
GO:1901564	organonitrogen compound metabolic process	BP	1.71E-02	165	1652
GO:0043161	proteasome-mediated ubiquitin-dependent protein catabolic process	BP	1.76E-02	34	274
GO:0009108	coenzyme biosynthetic process	BP	1.77E-02	16	106
GO:0015711	organic anion transport	BP	1.78E-02	27	207
GO:0044247	cellular polysaccharide catabolic process	BP	1.81E-02	8	40
GO:0009314	response to radiation	BP	1.83E-02	26	198
GO:0009135	purine nucleoside diphosphate metabolic process	BP	1.87E-02	11	64
GO:0009179	purine ribonucleoside diphosphate metabolic process	BP	1.87E-02	11	64
GO:0009185	ribonucleoside diphosphate metabolic process	BP	1.87E-02	11	64
GO:0006081	cellular aldehyde metabolic process	BP	1.89E-02	9	48
GO:0031497	chromatin assembly	BP	1.89E-02	9	48
GO:0010252	auxin homeostasis	BP	1.90E-02	5	19
GO:0005737	cytoplasm	CC	1.93E-02	483	5225
GO:0048037	cofactor binding	MF	1.94E-02	62	558
GO:0010498	proteasomal protein catabolic process	BP	1.94E-02	34	276
GO:0071310	cellular response to organic substance	BP	2.01E-02	39	326
GO:0036402	proteasome-activating ATPase activity	MF	2.02E-02	4	13
GO:0051513	regulation of monopolar cell growth	BP	2.06E-02	2	3
GO:0004604	phosphoadenylyl-sulfate reductase (thioredoxin) activity	MF	2.06E-02	2	3
GO:0019521	D-gluconate metabolic process	BP	2.06E-02	2	3
GO:0015928	fucosidase activity	MF	2.06E-02	2	3
GO:0004560	alpha-L-fucosidase activity	MF	2.06E-02	2	3
GO:0033353	S-adenosylmethionine cycle	BP	2.06E-02	2	3
GO:0006430	lysyl-tRNA aminoacylation	BP	2.06E-02	2	3
GO:0004824	lysine-tRNA ligase activity	MF	2.06E-02	2	3
GO:0019419	sulfate reduction	BP	2.06E-02	2	3
GO:0004664	prephenate dehydratase activity	MF	2.06E-02	2	3
GO:0017077	oxidative phosphorylation uncoupler activity	MF	2.06E-02	2	3
GO:1902882	regulation of response to oxidative stress	BP	2.06E-02	2	3
GO:1901031	regulation of response to reactive oxygen species	BP	2.06E-02	2	3
GO:0019878	lysine biosynthetic process via aminoadipic acid	BP	2.06E-02	2	3
GO:0042073	intraciliary transport	BP	2.06E-02	2	3
GO:0098840	protein transport along microtubule	BP	2.06E-02	2	3
GO:0099118	microtubule-based protein transport	BP	2.06E-02	2	3
GO:0035721	intraciliary retrograde transport	BP	2.06E-02	2	3
GO:0030991	intraciliary transport particle A	CC	2.06E-02	2	3
GO:0050896	response to stimulus	BP	2.09E-02	288	3025

GO:0009414	response to water deprivation	BP	2.09E-02	11	65
GO:0031225	anchored component of membrane	CC	2.10E-02	18	126
GO:0051287	NAD binding	MF	2.12E-02	13	82
GO:0008514	organic anion transmembrane transporter activity	MF	2.13E-02	22	163
GO:0060560	developmental growth involved in morphogenesis	BP	2.14E-02	9	49
GO:1901576	organic substance biosynthetic process	BP	2.16E-02	355	3781
GO:0015672	monovalent inorganic cation transport	BP	2.28E-02	37	309
GO:0005829	cytosol	CC	2.34E-02	89	847
GO:0031597	cytosolic proteasome complex	CC	2.36E-02	5	20
GO:0009860	pollen tube growth	BP	2.36E-02	5	20
GO:0015865	purine nucleotide transport	BP	2.36E-02	5	20
GO:0015868	purine ribonucleotide transport	BP	2.36E-02	5	20
GO:0051503	adenine nucleotide transport	BP	2.36E-02	5	20
GO:0019900	kinase binding	MF	2.39E-02	6	27
GO:0051130	positive regulation of cellular component organization	BP	2.39E-02	8	42
GO:0009163	nucleoside biosynthetic process	BP	2.39E-02	8	42
GO:0042455	ribonucleoside biosynthetic process	BP	2.39E-02	8	42
GO:0016860	intramolecular oxidoreductase activity	MF	2.42E-02	9	50
GO:0043255	regulation of carbohydrate biosynthetic process	BP	2.51E-02	3	8
GO:0015002	heme-copper terminal oxidase activity	MF	2.51E-02	3	8
GO:0016675	oxidoreductase activity, acting on a heme group of donors	MF	2.51E-02	3	8
GO:0016676	oxidoreductase activity, acting on a heme group of donors, oxygen as acceptor	MF	2.51E-02	3	8
GO:0004129	cytochrome-c oxidase activity	MF	2.51E-02	3	8
GO:1901677	phosphate transmembrane transporter activity	MF	2.51E-02	3	8
GO:0000275	mitochondrial proton-transporting ATP synthase complex, catalytic core F(1)	CC	2.51E-02	3	8
GO:0019320	hexose catabolic process	BP	2.51E-02	3	8
GO:0006556	S-adenosylmethionine biosynthetic process	BP	2.51E-02	3	8
GO:0033180	proton-transporting V-type ATPase, V1 domain	CC	2.51E-02	3	8
GO:0005471	ATP:ADP antiporter activity	MF	2.51E-02	3	8
GO:0022900	electron transport chain	BP	2.60E-02	14	93
GO:0006720	isoprenoid metabolic process	BP	2.63E-02	15	102
GO:0009423	chorismate biosynthetic process	BP	2.64E-02	4	14
GO:0045261	proton-transporting ATP synthase complex, catalytic core F(1)	CC	2.64E-02	4	14
GO:0016868	intramolecular transferase activity, phosphotransferases	MF	2.64E-02	4	14
GO:0015217	ADP transmembrane transporter activity	MF	2.64E-02	4	14
GO:0018210	peptidyl-threonine modification	BP	2.64E-02	4	14

GO:0018107	peptidyl-threonine phosphorylation	BP	2.64E-02	4	14
GO:0045330	aspartyl esterase activity	MF	2.66E-02	10	59
GO:0000096	sulfur amino acid metabolic process	BP	2.72E-02	9	51
GO:0031968	organelle outer membrane	CC	2.72E-02	9	51
GO:0009826	unidimensional cell growth	BP	2.72E-02	8	43
GO:0015291	secondary active transmembrane transporter activity	MF	2.79E-02	32	264
GO:0005992	trehalose biosynthetic process	BP	2.82E-02	6	28
GO:0009225	nucleotide-sugar metabolic process	BP	2.82E-02	6	28
GO:0048588	developmental cell growth	BP	2.82E-02	6	28
GO:0022890	inorganic cation transmembrane transporter activity	MF	2.83E-02	38	324
GO:0044815	DNA packaging complex	CC	2.84E-02	11	68
GO:0016903	oxidoreductase activity, acting on the aldehyde or oxo group of donors	MF	2.84E-02	11	68
GO:0008540	proteasome regulatory particle, base subcomplex	CC	2.89E-02	5	21
GO:0006098	pentose-phosphate shunt	BP	2.89E-02	5	21
GO:0071705	nitrogen compound transport	BP	2.96E-02	74	697
GO:0008134	transcription factor binding	MF	3.05E-02	9	52
GO:0034728	nucleosome organization	BP	3.05E-02	9	52
GO:0009064	glutamine family amino acid metabolic process	BP	3.09E-02	8	44
GO:0090407	organophosphate biosynthetic process	BP	3.18E-02	31	257
GO:0006631	fatty acid metabolic process	BP	3.26E-02	22	170
GO:0005871	kinesin complex	CC	3.28E-02	10	61
GO:0009119	ribonucleoside metabolic process	BP	3.28E-02	10	61
GO:0046658	anchored component of plasma membrane	CC	3.28E-02	16	114
GO:0009651	response to salt stress	BP	3.31E-02	14	96
GO:0005991	trehalose metabolic process	BP	3.31E-02	6	29
GO:0016126	sterol biosynthetic process	BP	3.31E-02	6	29
GO:0022804	active transmembrane transporter activity	MF	3.32E-02	60	554
GO:0070413	trehalose metabolism in response to stress	BP	3.37E-02	4	15
GO:0005753	mitochondrial proton-transporting ATP synthase complex	CC	3.37E-02	4	15
GO:1990351	transporter complex	CC	3.37E-02	4	15
GO:0015867	ATP transport	BP	3.37E-02	4	15
GO:0006333	chromatin assembly or disassembly	BP	3.41E-02	9	53
GO:0045087	innate immune response	BP	3.41E-02	9	53
GO:0044437	vacuolar part	CC	3.42E-02	28	229
GO:0005774	vacuolar membrane	CC	3.42E-02	28	229
GO:0015932	nucleobase-containing compound transmembrane transporter activity	MF	3.47E-02	7	37
GO:0043900	regulation of multi-organism process	BP	3.48E-02	5	22
GO:0070566	adenylyltransferase activity	MF	3.48E-02	5	22
GO:0016101	diterpenoid metabolic process	BP	3.48E-02	5	22

GO:1901264	carbohydrate derivative transport	BP	3.49E-02	8	45
GO:0000302	response to reactive oxygen species	BP	3.49E-02	8	45
GO:0016049	cell growth	BP	3.52E-02	12	79
GO:0051053	negative regulation of DNA metabolic process	BP	3.53E-02	3	9
GO:0010112	regulation of systemic acquired resistance	BP	3.53E-02	3	9
GO:0010167	response to nitrate	BP	3.53E-02	3	9
GO:0004478	methionine adenosyltransferase activity	MF	3.53E-02	3	9
GO:0051046	regulation of secretion	BP	3.53E-02	3	9
GO:1903530	regulation of secretion by cell	BP	3.53E-02	3	9
GO:0017157	regulation of exocytosis	BP	3.53E-02	3	9
GO:0019722	calcium-mediated signaling	BP	3.53E-02	3	9
GO:0034637	cellular carbohydrate biosynthetic process	BP	3.60E-02	24	191
GO:0098662	inorganic cation transmembrane transport	BP	3.61E-02	38	330
GO:0030599	pectinesterase activity	MF	3.62E-02	10	62
GO:0005516	calmodulin binding	MF	3.76E-02	11	71
GO:0006955	immune response	BP	3.79E-02	9	54
GO:0043648	dicarboxylic acid metabolic process	BP	3.83E-02	12	80
GO:0005388	calcium-transporting ATPase activity	MF	3.85E-02	6	30
GO:0051087	chaperone binding	MF	3.85E-02	6	30
GO:0019682	glyceraldehyde-3-phosphate metabolic process	BP	3.85E-02	6	30
GO:0009926	auxin polar transport	BP	3.85E-02	6	30
GO:0016830	carbon-carbon lyase activity	MF	3.86E-02	13	89
GO:0015849	organic acid transport	BP	3.89E-02	20	154
GO:0046942	carboxylic acid transport	BP	3.89E-02	20	154
GO:0042814	monopolar cell growth	BP	3.89E-02	2	4
GO:0051510	regulation of unidimensional cell growth	BP	3.89E-02	2	4
GO:0015929	hexosaminidase activity	MF	3.89E-02	2	4
GO:0004563	beta-N-acetylhexosaminidase activity	MF	3.89E-02	2	4
GO:0072583	clathrin-dependent endocytosis	BP	3.89E-02	2	4
GO:0008215	spermine metabolic process	BP	3.89E-02	2	4
GO:0046499	S-adenosylmethioninamine metabolic process	BP	3.89E-02	2	4
GO:0006597	spermine biosynthetic process	BP	3.89E-02	2	4
GO:0006557	S-adenosylmethioninamine biosynthetic process	BP	3.89E-02	2	4
GO:0004014	adenosylmethionine decarboxylase activity	MF	3.89E-02	2	4
GO:0019520	aldonic acid metabolic process	BP	3.89E-02	2	4
GO:0019464	glycine decarboxylation via glycine cleavage system	BP	3.89E-02	2	4
GO:0005960	glycine cleavage complex	CC	3.89E-02	2	4
GO:0048598	embryonic morphogenesis	BP	3.89E-02	2	4
GO:0019673	GDP-mannose metabolic process	BP	3.89E-02	2	4
GO:0030990	intraciliary transport particle	CC	3.89E-02	2	4
GO:0046439	L-cysteine metabolic process	BP	3.89E-02	2	4
GO:0046498	S-adenosylhomocysteine metabolic process	BP	3.89E-02	2	4

GO:0017101	aminoacyl-tRNA synthetase multienzyme complex	CC	3.89E-02	2	4
GO:0008970	phosphatidylcholine 1-acylhydrolase activity	MF	3.89E-02	2	4
GO:0004128	cytochrome-b5 reductase activity, acting on NAD(P)H	MF	3.89E-02	2	4
GO:0045912	negative regulation of carbohydrate metabolic process	BP	3.89E-02	2	4
GO:1905156	negative regulation of photosynthesis	BP	3.89E-02	2	4
GO:1901659	glycosyl compound biosynthetic process	BP	3.92E-02	8	46
GO:1901505	carbohydrate derivative transporter activity	MF	3.96E-02	7	38
GO:0009914	hormone transport	BP	3.96E-02	7	38
GO:0035639	purine ribonucleoside triphosphate binding	MF	4.04E-02	266	2825
GO:0016491	oxidoreductase activity	MF	4.05E-02	185	1920
GO:0009653	anatomical structure morphogenesis	BP	4.07E-02	22	174
GO:0015171	amino acid transmembrane transporter activity	MF	4.10E-02	15	108
GO:0004721	phosphoprotein phosphatase activity	MF	4.12E-02	20	155
GO:0006094	gluconeogenesis	BP	4.15E-02	5	23
GO:0006558	L-phenylalanine metabolic process	BP	4.15E-02	5	23
GO:1902221	erythrose 4-phosphate/phosphoenolpyruvate family amino acid metabolic process	BP	4.15E-02	5	23
GO:0009932	cell tip growth	BP	4.15E-02	5	23
GO:0006862	nucleotide transport	BP	4.15E-02	5	23
GO:0050662	coenzyme binding	MF	4.16E-02	40	354
GO:0016874	ligase activity	MF	4.20E-02	24	194
GO:0019867	outer membrane	CC	4.20E-02	9	55
GO:0080044	quercetin 7-O-glucosyltransferase activity	MF	4.28E-02	26	214
GO:0080043	quercetin 3-O-glucosyltransferase activity	MF	4.28E-02	26	214
GO:0009814	defense response, incompatible interaction	BP	4.44E-02	6	31
GO:0071944	cell periphery	CC	4.53E-02	200	2094
GO:0005342	organic acid transmembrane transporter activity	MF	4.65E-02	18	138
GO:0046943	carboxylic acid transmembrane transporter activity	MF	4.65E-02	18	138
GO:0006865	amino acid transport	BP	4.71E-02	15	110
GO:0044455	mitochondrial membrane part	CC	4.71E-02	15	110
GO:0004040	amidase activity	MF	4.73E-02	3	10
GO:0006123	mitochondrial electron transport, cytochrome c to oxygen	BP	4.73E-02	3	10
GO:0009817	defense response to fungus, incompatible interaction	BP	4.73E-02	3	10
GO:0016161	beta-amylase activity	MF	4.73E-02	3	10
GO:0102229	amylopectin maltohydrolase activity	MF	4.73E-02	3	10
GO:0015695	organic cation transport	BP	4.73E-02	3	10
GO:0019932	second-messenger-mediated signaling	BP	4.73E-02	3	10

GO:0000394	RNA splicing, via endonucleolytic cleavage and ligation	BP	4.73E-02	3	10
GO:1903825	organic acid transmembrane transport	BP	4.78E-02	17	129
GO:1905039	carboxylic acid transmembrane transport	BP	4.78E-02	17	129
GO:0005874	microtubule	CC	4.79E-02	14	101
GO:0006534	cysteine metabolic process	BP	4.88E-02	5	24
GO:0045259	proton-transporting ATP synthase complex	CC	4.88E-02	5	24
GO:0019319	hexose biosynthetic process	BP	4.88E-02	5	24
GO:0046364	monosaccharide biosynthetic process	BP	4.88E-02	5	24

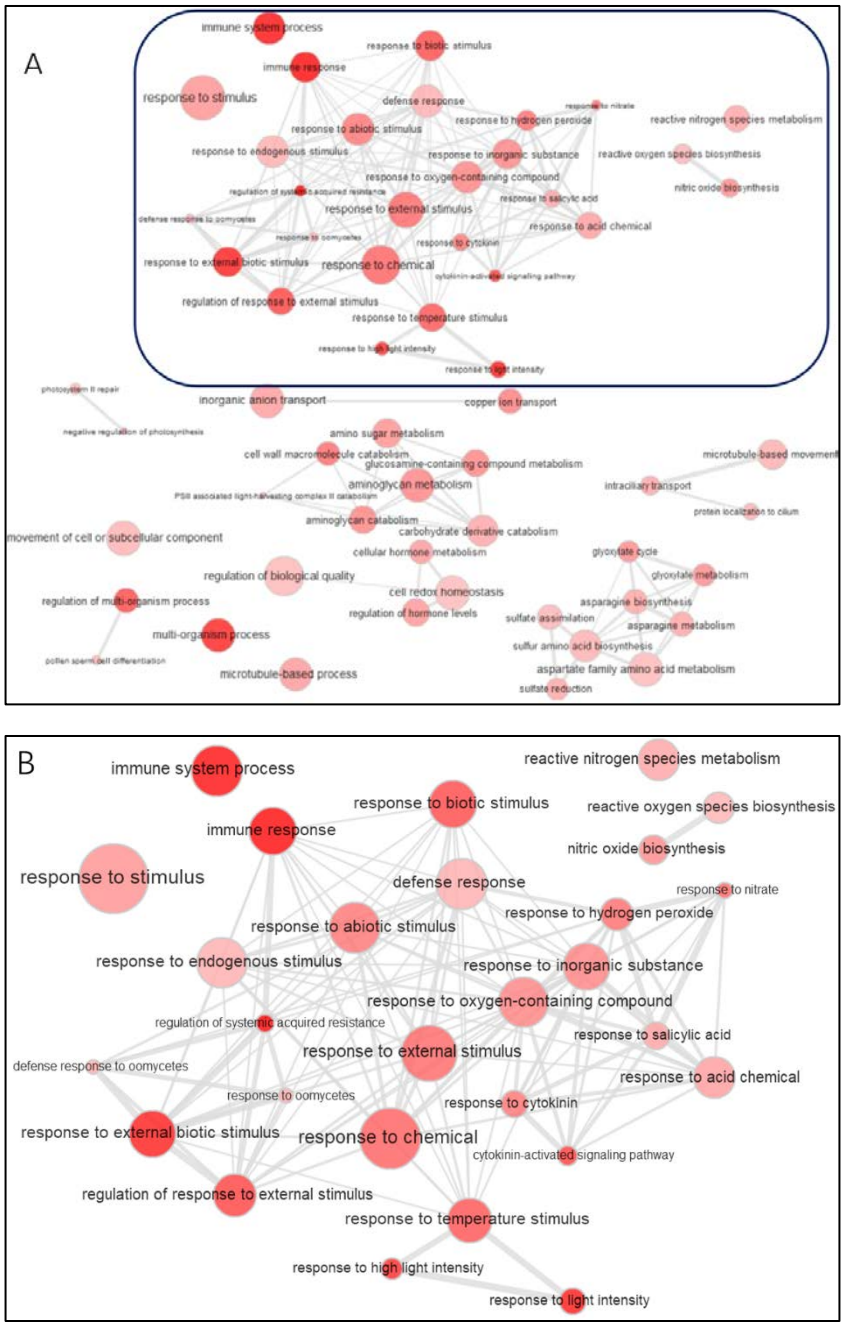

Supplementary Fig S1. Network visualisation of biological process in drought treatment.

(A) Network visualisation for all GO terms. (B) Network visualisation for the focused GO terms. Bubble colour represents the P-value of GO terms; darker colour implies more significant terms. Circle size represents the frequency of GO terms in the Uniprot database. Highly similar GO terms are linked together in the graph, where the line width implies the degree of similarity following published REVIGO protocol (http://revigo.irb.hr).

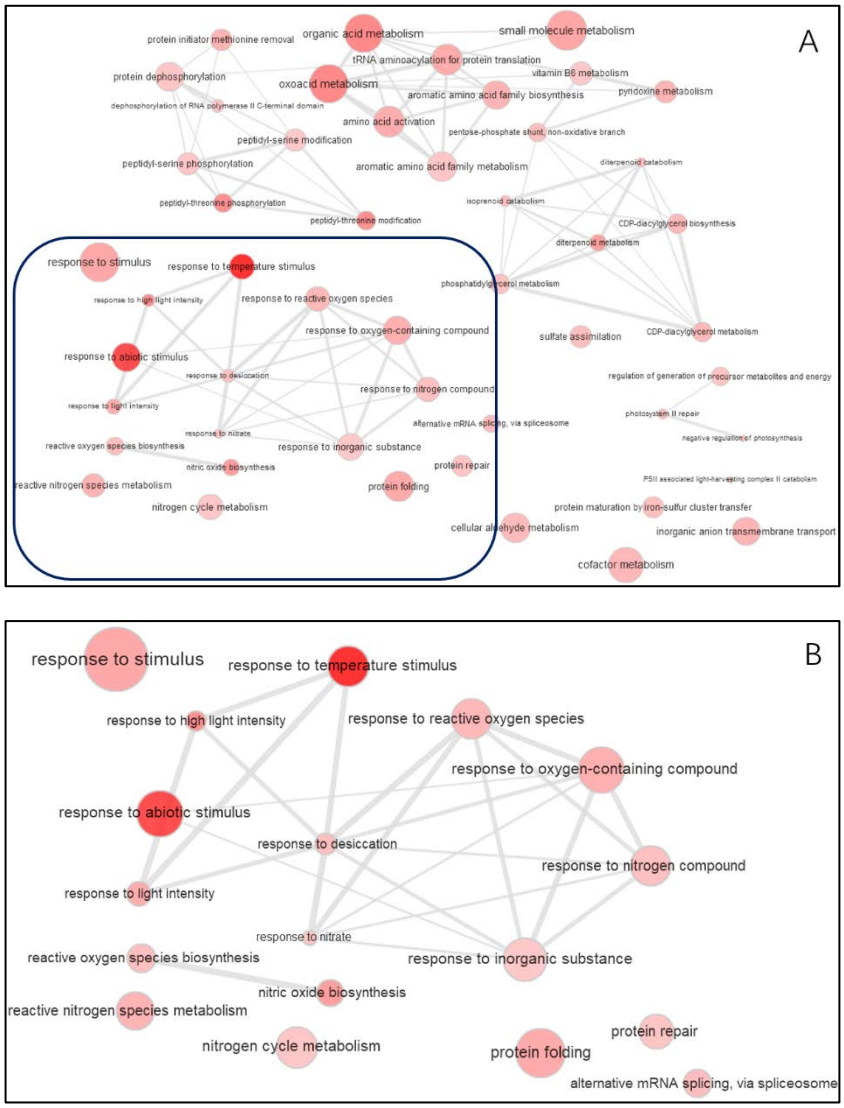

Supplementary Fig S2. Network visualisation of biological process in heat treatment. (A) Network visualisation for all GO terms. (B) Network visualisation for the focused GO terms. Bubble colour represents the P-value of GO terms; darker colour implies more significant terms. Circle size represents the frequency of GO terms in the Uniprot database. Highly similar GO terms are linked together in the graph, where the line width implies the degree of similarity following published REVIGO protocol (http://revigo.irb.hr).

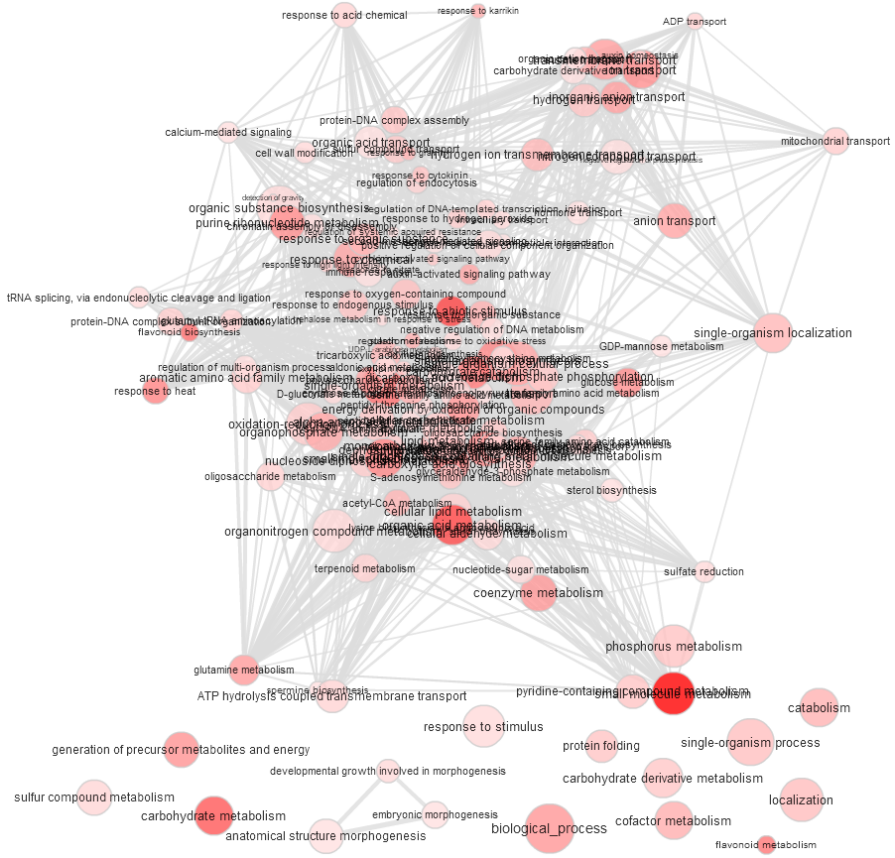

Supplementary Fig S3. Network visualisation of biological process in drought/heat treatment. Bubble colour represents the P-value of GO terms; darker colour implies more significant terms. Circle size represents the frequency of GO terms in the Uniprot database. Highly similar GO terms are linked together in the graph, where the line width implies the degree of similarity following published REVIGO protocol (http://revigo.irb.hr).